ChemPubSoc Europe

DOI: 10.1002/cmdc.201402075

# Development of Novel Selective Peptidomimetics Containing a Boronic Acid Moiety, Targeting the 20S Proteasome as Anticancer Agents

Kety Scarbaci,[b] Valeria Troiano,[b] Roberta Ettari,*[a] Andrea Pinto,[a] Nicola Micale,[b] Carmen Di Giovanni,[c] Carmen Cerchia,[c] Tanja Schirmeister,[d] Ettore Novellino,[c] Antonio Lavecchia,*[c] Maria Zappalà,[b] and Silvana Grasso[e]

This paper describes the design, synthesis, and biological evaluation of peptidomimetic boronates as inhibitors of the 20S proteasome, a validated target in the treatment of multiple myeloma. The synthesized compounds showed a good inhibitory profile against the ChT-L activity of 20S proteasome. Compounds bearing a β-alanine residue at the P2 position were the most active, that is, 3-ethylphenylamino and 4-methoxyphenylamino (*R*)-1-{3-[4-(substituted)-2-oxopyridin-1(2*H*)-yl]propanamido}-3-methylbutylboronic acids (**3c** and **3d**, respectively), and these derivatives showed inhibition constants ($K_i$) of 17 and 20 nM, respectively. In addition, they co-inhibited post glutamyl peptide hydrolase activity (**3c**, $K_i = 2.57$ μM; **3d**, $K_i = 3.81$ μM). No inhibition was recorded against the bovine pancreatic α-chymotrypsin, which thus confirms the selectivity towards the target enzyme. Docking studies of **3c** and related inhibitors into the yeast proteasome revealed the structural basis for specificity. The evaluation of growth inhibitory effects against 60 human tumor cell lines was performed at the US National Cancer Institute. Among the selected compounds, **3c** showed 50% growth inhibition ($GI_{50}$) values at the sub-micromolar level on all cell lines.

## Introduction

The 20S proteasome is an essential component of the adenosine triphosphate-dependent proteolytic pathway in eukaryotic cells, and it plays a key role in the degradation of most cellular proteins. It has a barrel-like structure and is composed of four stacked rings, each of which contains seven subunits. Whereas the two inner rings contain seven β subunits (β1–β7), the two outer rings are characterized by α subunits (α1–α7).[1] The catalytic activities of the proteasome are classified into three major categories: chymotrypsin-like (ChT-L), trypsin-like (T-L), and post glutamyl peptide hydrolase or caspase-like (PGPH or C-L), associated with the β5, β2, and β1 subunits that cleave after hydrophobic, basic, and acidic residues, respectively.[2] Defects in proteasome activity can induce tumor development owing to anarchic cell proliferation, and thus a promising strategy for cancer treatment is the inhibition ChT-L activity.[3] Recent studies clearly point out that an efficient reduction in abnormal proteasome activity can be achieved only by the simultaneous inhibition of ChT-L activity, together with a second active site,[4] whereas inhibition of all three catalytic subunits is strongly cytotoxic.

Over the last years our research group has been involved in the development of peptidomimetic 20S proteasome inhibitors,[5,6] structurally related to bortezomib (Velcade, Figure 1), the first proteasome inhibitor approved by the US Food and Drug Administration (FDA) for the treatment of multiple myeloma[7] and mantle cell lymphoma.[8] Although bortezomib has been shown to provide significant benefits to patients with multiple myeloma in clinical trials, its efficacy and its administration have been limited by toxic side effects,[7] the most severe ones include hematological toxicity and peripheral neuropathy, characterized by decreased sensation, paresthesia, and a high rate of shingles. As a matter of fact, bortezomib is able to activate the mitochondrial-based apoptotic pathway, in which mitochondrial and endoplasmic reticulum damage may play a key role in bortezomib-induced side effects.

Taking into account all of these problems, the development of peptidomimetics could present many pharmacokinetic and pharmacodynamic advantages, as also described in the case of selective peptidomimetic 20S proteasome inhibitors.[9] This strategy can be accomplished, for example, by simple replace-

[a] *Dr. R. Ettari, Dr. A. Pinto*
*Dipartimento di Scienze del Farmaco e Prodotti per la Salute*
*Università degli Studi di Messina, Viale Annunziata, 98168 Messina (Italy)*
*E-mail: roberta.ettari@unimi.it*

[b] *Dr. K. Scarbaci, Dr. V. Troiano, Dr. N. Micale, Prof. M. Zappalà*
*Dipartimento di Scienze Farmaceutiche*
*Università degli Studi di Milano, Via Mangiagalli, 25, 20133 Milano (Italy)*

[c] *Dr. C. Di Giovanni, Dr. C. Cerchia, Prof. E. Novellino, Prof. A. Lavecchia*
*Drug Discovery Laboratory, Dipartimento di Farmacia*
*Università degli Studi di Napoli, Via Montesano 49, 80131 Napoli (Italy)*
*E-mail: antonio.lavecchia@unina.it*

[d] *Prof. Dr. T. Schirmeister*
*Institut für Pharmazie & Biochemie, Johannes Gutenberg Universität Mainz*
*Staudinger Weg 5, 55099 Mainz (Germany)*

[e] *Prof. S. Grasso*
*Dipartimento di Scienze Chimiche, Università degli Studi di Messina*
*Via F. Stagno D'Alcontres 31, S. Agata, 98166 Messina (Italy)*

  

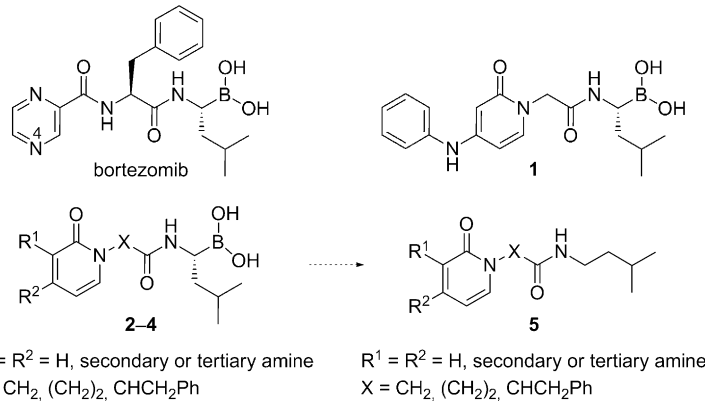


**Figure 1.** Structures of bortezomib, lead compound **1**, boronates **2**–**4**, and amides **5**.

ment of natural amino acids with unnatural amino acids or by the introduction of a rigid scaffold into peptide sequences in such a way as to lock a defined conformation of the peptide.[10–12]

In this context, we recently developed conformationally constrained pseudopeptide boronates[6] by using bortezomib as a lead compound that are characterized by a 1*H*-pyridin-2-one ring at P3 as a constrained motif. Overall, this new class of peptidomimetics showed a promising inhibitory profile by blocking two out of three proteolytic activities of the proteasome with preference for β5 subunits. In this work, starting from most active peptidomimetic boronate **1** (Figure 1), we designed boronic acids **2**–**4** (Figure 1) in which the 1*H*-pyridin-2-one ring was maintained in view of its ability to enclose the amide moiety of the pyrazinamide of bortezomib.

According to the attested ability of the N4 atom of the pyrazine nucleus of bortezomib to establish a H-bond with the protonated D114 moiety of the β6 subunit,[13] a highly conserved residue in mammals, we maintained a H-bond acceptor at the 4-position of the pyridone nucleus in view of the already demonstrated ability of the NH group of the 4-phenylamino substituent in **1** to form a H-bond with the side chain of this residue.[6] A variety of secondary and tertiary amino groups (e.g., phenylamino, 3-ethylphenylamino, 4-methoxyphenylamino, benzylamino, piperidin-1-yl, and 4-methylpiperazin-1-yl) were introduced in that position with the aim to establish a trend of reactivity. At the same time, 3-amino-substituted pyridone analogues were developed to compare their binding mode and their ability to interact with β6-D114. Additional structural modifications were the incorporation of different sterically hindered residues at the P2 position, such as phenylalanine in analogy to the structure of bortezomib and β-alanine, taking into consideration that several dipeptidyl boronic acids constructed from β-amino acids are endowed with a good profile in terms of proteasome inhibition, cytotoxic activity versus hematologic tumor cell lines, and pharmacokinetic properties.[14,15] The Leu-boronic electrophilic moiety was maintained as a warhead for its ability to reversibly interact with the N-terminal catalytic active site T1O$^{\gamma}$. In this regard, whereas irreversible blockage of an enzyme should be advantageous for parasitic targets,[16–19] on the contrary in the case of cancer treatment or immunologically related diseases, reversible or noncovalent inhibition would be desirable. As a matter of fact, to overcome all inherent drawbacks related to covalent inhibition (i.e., off-target interactions), some research groups have focused their efforts on the identification of noncovalent proteasome inhibitors with specificity for ChT-L subunits.[20] Generally, this type of inhibitor binds the active site by means of a hydrogen-bonding network involving the same amino acid residues of the covalent inhibitors (i.e., T21, G47, and A49).[21] In this context, the identification of a series of amides (i.e., **5a**–**h**) as byproducts in the synthetic route to the boronates also focused our attention on these promising noncovalent inhibitors. On the basis of our previous findings on a number of analogous amides as proteasome inhibitors[22] and according to recent literature data,[23] obtained compounds **5** were evaluated for their inhibitory properties against the three catalytic activities of 20S proteasome.

The covalent and noncovalent binding modes of the designed inhibitors were clarified through docking experiments by using the crystal structure of the yeast 20S proteasome. Furthermore, growth inhibitory effects of both the boronates and the amides were evaluated at the US National Cancer Institute (NCI) against 60 human tumor cell lines derived from 9 neoplastic diseases.

## Results and Discussion

### Chemistry

For the synthesis of pyridone scaffolds **11a**–**i** (Scheme 1), the first step of the synthetic pathway was the nucleophilic aromatic substitution reaction of 2-halopyridines **6** and **7** with benzyl alcohol in the presence of potassium hydride to afford benzyl esters **8** and **9**. The introduction of the suitable amine at the 3- or 4-position of 2-benzyloxypyridines **8** and **9** was performed by microwave-assisted Buchwald–Hartwig amination[24] in the presence of the suitable amine, $Pd_2(dba)_3$ as the catalyst (dba = dibenzylideneacetone), and DavePhos [2-dicyclohexylphosphino-2′-(*N*,*N*-dimethylamino)biphenyl] as the ligand system, which provided amino-substituted 2-benzyloxypyridines **10a**–**i** in high yields. Then debenzylation accomplished by palladium-catalyzed hydrogenation afforded amino-substituted 1*H*-pyridin-2-ones **11a**–**i**.

Pyridones **11** were then *N*-alkylated with ethyl bromoacetate, methyl 3-bromopropionate, or 2-trifluoromethanesulfonyloxy-3-phenylpropionic acid methyl ester at convenience in the presence of NaH to obtain esters **12a**–**p** (Scheme 2). Coupling reactions between corresponding acids **13a**–**p**, obtained by alkaline hydrolysis, and pinanediol leucine boronate (**14**)[6] in the presence of 1-ethyl-3-(3-dimethylaminopropyl)carbodiimide hydrochloride (EDC·HCl), hydroxybenzotriazole (HOBt), and *N*,*N*-diisopropylethylamine (DIPEA) afforded pinanediol esters **15a**–**p** (Scheme 2), which were employed without any further purification in the transesterification reaction with isobutylboronic

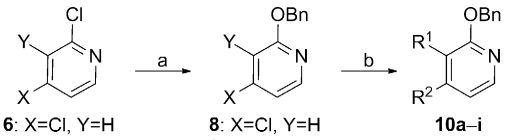


| | $R^1$ | $R^2$ |
|---|---|---|
| **a** | H | H |
| **b** | H | phenylamino |
| **c** | H | 3-ethylphenylamino |
| **d** | H | 4-methoxyphenylamino |
| **e** | H | benzylamino |
| **f** | H | piperidin-1-yl |
| **g** | H | methylpiperazin-1-yl |
| **h** | phenylamino | H |
| **i** | piperidin-1-yl | H |

**Scheme 1.** *Reagents and conditions*: a) BnOH, KH, THF, RT, 18 h, $N_2$, 87–96%; b) $Pd_2(dba)_3$, DavePhos or 2,2′-bis(diphenylphosphino)-1,1′-binaphthyl (BINAP), suitable amine, *t*BuONa, toluene, microwave, 120–150 °C, 15 min, $N_2$, 83–89%; c) $H_2$, 10% Pd/C, MeOH/EtOAc (2:1), RT, 2 h, 95–99% or $BBr_3$, $CH_2Cl_2$, −78 °C, 4 h, 99%.

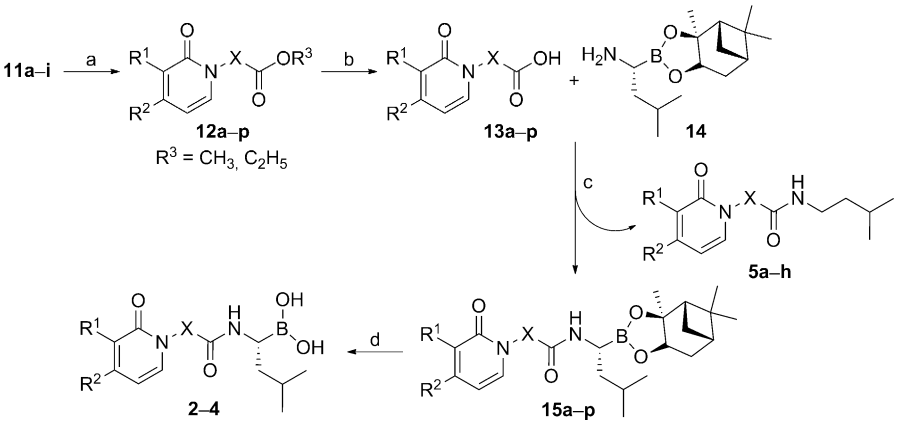


**Scheme 2.** *Reagents and conditions*: a) NaH, DMF, 0 °C, 1 h; then ethyl bromoacetate, methyl 3-bromopropionate, or 2-trifluoromethanesulfonyloxy-3-phenyl-propionic acid methyl ester, RT, 2 or 12 h, $N_2$, 40-83%; b) 1 N LiOH, EtOH, 0 °C→RT, 4 h, 95–99%; c) HOBt, $CH_2Cl_2$, −5 °C, 20 min, then EDC·HCl, DIPEA, pinanediol L-leucine boronate (**14**), −15 °C→RT, 3 h, 70–87%; d) *i*BuB(OH)$_2$, 1 N HCl, MeOH/*n*-hexane (1:1), RT, 18 h, 37–70%.

dopeptides **2**–**4** did not show any inhibition, with the exception of **2b** (dissociation constant ($K_i$) = 16.36 μM), showing a certain degree of target selectivity.

Synthesized boronates **2**–**4** were then tested for their inhibitory properties on purified constitutive 20S proteasome isolated from human erythrocytes by using the appropriate fluorogenic substrate for each one of the proteolytic activities (Suc-Leu-Leu-Val-Tyr-AMC for ChT-L, Boc-Leu-Arg-Arg-AMC for T-L, CBz-Leu-Leu-Glu-AMC for PGPH; Suc = succinyl, Boc = *tert*-butoxycarbonyl, CBz = benzyloxycarbonyl, AMC = aminomethylcoumarin). First, compounds underwent a preliminary screening for ChT-L activity at 20 μM by using an equivalent volume of dimethyl sulfoxide (DMSO) as a negative control. The screening showed that all compounds, with the exceptions of **2c**, **3e**, and **4b**, inhibited more than 40% of the enzyme activity.

Continuous assays were then performed [progress curve method, at seven different concentrations ranging from those that minimally inhibited to those that fully inhibited the enzyme (Figure 2)] to determine the $K_i$ values (Figure 3), which are reported in Table 1. All compounds were proven to inhibit the ChT-L activity of 20S proteasome with $K_i$ values in the submicromolar/micromolar range.

All compounds **2** are less potent than lead compound **1**: the introduction of a substituent on the PhNH moiety (i.e., **2a** and **2b**), as well as its shift to the 3-position (i.e., **2d**), led to a decrease in the inhibitory activity. Overall, compounds **3** bearing a β-alanine residue at P2 were the most potent inhibitors, according to the good activity of dipeptidyl boronic acid proteasome inhibitors having β-amino acid residues, which were reacid under acid conditions to provide desired boronic acids **2**–**4**.

As above mentioned, byproducts **5** were identified in the reported synthesis route. Although amides are minor reaction products, their formation from the corresponding boronates is quite often observed in basic aqueous solutions.[25] In detail, the coupling reaction between carboxylic acids **13** and pinanediol leucine boronate (**14**) led to the formation of amides **5** obtained by spontaneous deboronation of boronic esters **15** (Scheme 2).

### Inhibitory effect on the ChT-L, T-L, and PGPH activities of human 20S proteasome

To check the selectivity of the synthesized compounds, they were tested against bovine pancreatic α-chymotrypsin; pseu-

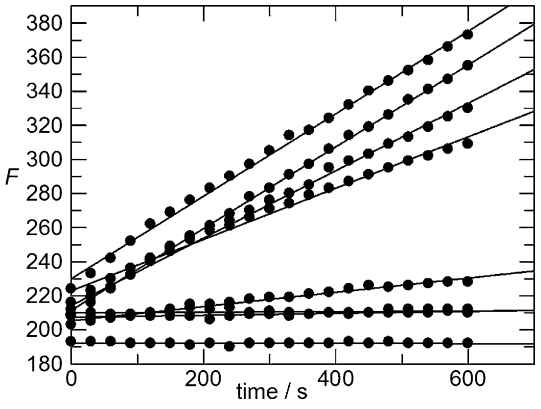


**Figure 2.** Progress curves of substrate hydrolysis in the presence of inhibitor **3c**. F = fluorescence units. Inhibitor concentrations (from top to bottom): 0, 0.1, 0.2, 0.5, 1.0, 5.0, 10.0, 20.0 μM.

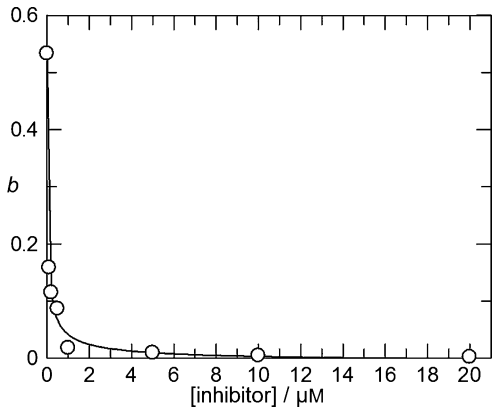


**Figure 3.** The slopes of the progress curve (*b*) from Figure 2 were plotted against the inhibitor concentrations and fitted to the four-parameter $IC_{50}$ equation. $K_i$ was obtained from Equation (1).

cently reported.[14,15] In this context, boronic acids **3c** and **3d** showed $K_i$ values of 17 and 20 nM, respectively, against ChT-L activity, which are quite comparable to the $K_i$ value of bortezomib (9.8 nM), which was tested under the same experimental conditions.

In derivatives **3**, the introduction of the phenylamino substituent on the pyridone nucleus positively affected the inhibitory activity (i.e., **3b** versus **3a**), whereas the position of this group did not seem to have a significant influence: the potencies of **3b** and **3g** are quite similar. Moreover, the presence of a small lipophilic substituent on the aromatic moiety (i.e., **3c** and **3d** versus **3b**) seems to be relevant.

For both derivatives **2** and **3**, the introduction of a tertiary amine at the C3 or C4 position of the heterocyclic nucleus, in particular of the piperidine ring (e.g., **3e**), was detrimental for ChT-L and PGPH inhibition. In compounds **4**, a Phe residue was introduced at the P2 site. To investigate the importance of the stereochemistry, we synthesized diastereoisomers **4a** and **4b** having the *S* and *R* configuration at this site. The presence for an (*S*)-Phe residue at the P2 site strongly improved the potency. Notably, compound **4a** proved to be a nanomolar inhibitor of the ChT-L activity of 20S proteasome ($K_i = 36$ nM), whereas its diastereoisomer **4b** was inactive.

The inhibitory activity towards the other two proteasome activities (i.e., T-L and PGPH), together with the selectivity of boronates **2**–**4** towards the target enzyme, determined by using bovine pancreatic α-chymotrypsin, was performed with the same method. None of the tested compounds showed any inhibition of the T-L activity at 20 μM, whereas six of the screened boronates, including the most active inhibitors **3c** and **3d**, inhibited the PGPH activity, although with $K_i$ one or two orders of magnitude higher than that reported for the inhibition of the β5 subunit (Table 1). According to the reported data,[4] the co-inhibition of the β5 subunit with either the β1 or β2 subunit is strongly desirable to enhance an antitumor response, and on the contrary, the co-inhibition of all proteasome subunits has been proven to be cytotoxic.

Concerning amides **5a**–**h**, the $K_i$ values were obtained according to the same methods described for boronates **2**–**4** (Table 2). In agreement with the discussed results regarding boronates **2**–**4**, amides bearing the amino group at the 4-position of the pyridone ring (i.e., **5a** and **5e**–**h**) were effective against ChT-L activity.

Among them, compound **5h** showed a promising inhibitory effect on ChT-L activity ($K_i = 0.44$ μM, one order of magnitude less than the others), which proved the effectiveness of the most-hindered phenylalanine residue. No inhibition was recorded against the PGPH and T-L activities at 20 μM concentration.

**Table 1.** Inhibition ChT-L and PGPH proteasome activities by boronates **1**–**4**.

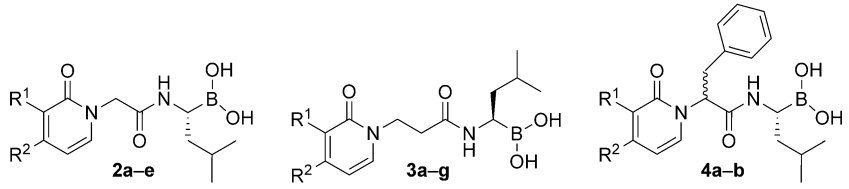


| Compd | $R^1$ | $R^2$ | $K_i$ [μM][a] or % inhibition ChT-L | PGPH |
|---|---|---|---|---|
| **1** | H | phenylamino | 0.098 ± 0.05 | 5.14 ± 1.10 |
| **2a** | H | 3-ethylphenylamino | 30% at 20 μM | n.i. |
| **2b** | H | 4-methoxyphenylamino | 0.23 ± 0.05 | 3.37 ± 1.62 |
| **2c** | H | benzylamino | n.i. | n.i. |
| **2d** | phenylamino | H | 40% at 20 μM | n.i. |
| **2e** | piperidin-1-yl | H | 13.09 ± 0.20 | n.i. |
| **3a** | H | H | 3.66 ± 0.60 | n.i. |
| **3b** | H | phenylamino | 0.13 ± 0.01 | 5.33 ± 0.04 |
| **3c** | H | 3-ethylphenylamino | 0.017 ± 0.012 | 2.57 ± 0.17 |
| **3d** | H | 4-methoxyphenylamino | 0.02 ± 0.01 | 3.81 ± 0.09 |
| **3e** | H | piperidin-1-yl | n.i. | n.i. |
| **3f** | H | 4-methylpiperazin-1-yl | 2.08 ± 1.03 | n.i. |
| **3g** | phenylamino | H | 0.19 ± 0.04 | 4.52 ± 0.27 |
| **4a** (*S*,Phe) | H | phenylamino | 0.036 ± 0.001 | n.i. |
| **4b** (*R*,Phe) | H | phenylamino | n.i. | n.i. |
| bortezomib | | | 0.009 ± 0.001 | n.d. |

[a] For $K_i$ values, data represent the mean ± SD of three independent determinations. n.d. = not determined; n.i. = no inhibition.

## Docking studies

To help interpret the structure–activity relationship (SAR) data and to gain a better understanding of how the described boronate and non-boronate inhibitors might bind to the 20S proteasome, we performed docking simulations of most active compounds **3c**, **3d**, **4a**, and **5h** into the binding pocket of the β5 subunit of the previously reported crystal structure of bortezomib bound to the yeast 20S proteasome (PDB ID: 2F16).[13] Given that inhibitors **3c**, **3d**, and **4a** covalently bind to the catalytic T1 residue in the β5 proteasome subunit through an ester bond, the covalent docking procedure

**Table 2.** Inhibition of ChT-L proteasome activity by amides **5a–h**.

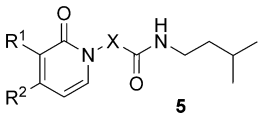

**5**

| Compd | $R^1$ | $R^2$ | X | $K_i$ [μM][a] ChT-L |
|---|---|---|---|---|
| **5a** | H | 4-methoxyphenylamino | $CH_2$ | 1.71 ± 0.71 |
| **5b** | phenylamino | H | $CH_2$ | n.i. |
| **5c** | piperidin-1-yl | H | $CH_2$ | n.i. |
| **5d** | H | H | $(CH_2)_2$ | n.i. |
| **5e** | H | phenylamino | $(CH_2)_2$ | 6.09 ± 1.07 |
| **5f** | H | 4-methoxyphenylamino | $(CH_2)_2$ | 1.89 ± 0.99 |
| **5g** | H | piperidin-1-yl | $(CH_2)_2$ | 3.62 ± 1.09 |
| **5h** | H | phenylamino | (*S*)-$CHCH_2Ph$ | 0.44 ± 0.13 |

[a] Data represent the mean ± SD of three independent determinations. n.i. = no inhibition.

provided by GOLD 5.2[26,27] was used for routine docking in which both the protein and the ligand contained the linking oxygen atom of T1 (Figure 4). This required that the structures of the ligands be prepared as their corresponding hydroxyl addition products with one open valence at the oxygen atom. The docking procedure confirmed that the boron atom of the ligands was indeed the site of reactivity with T1. With regard to non-boronate-containing **5h**, the conventional GOLD docking procedure was performed (Figure 5).

The binding mode of **3c**, **3d**, and **4a** was similar to that of previously published proteasome inhibitor **1**[6] and bortezomib.[13] As depicted in Figure 2, the inhibitors were found to adopt a β conformation and to fill the gap between strands S2 and S4 by forming H-bonds with residues T21 and G47, and for **4a** only, A49 of the β5 subunit. The isopentyl substituent of all the inhibitors was found to project into the S1 pocket by adopting the same spatial arrangement of the P1 leucine side chain of bortezomib. K33, M45, A49, and V31 of subunit β5 stabilized the P1 isopentyl moiety through van der Waals interactions. The phenylalanine group of **4a**, which is missing in **3c** and **3d**, was not in contact with the protein and pointed towards the S2 pocket, a large cavity able to accept space-demanding side-chain residues. The 4-phenylamino substituents of the inhibitors stretched out into the subunit-specific S3 pocket and were in close contact with the residues of the adjacent β6 subunit with their N atom H-bonded to the OH group of β6-D114. This result is in consonance with biochemical investigations showing that the size and length of the P3 side chain is crucial for activity.[28,29] Among the peptidomimetic boronates tested, the 3-ethyl- and 4-methoxyphenylamino substituents at P3 (i.e., compounds **3c** and **3d**) gave the most active inhibition. The structure of the 20S proteasome shows that the β5 and β6 subunits constitute the binding cleft of the S3 specificity pocket, which is able to accommodate long and bulky substituents. The docking results revealed that the substituted phenylamino moiety of **3c** and **3d** were able to fit perfectly into the S3 pocket of the proteasome by making hydrophobic interactions with the A27 residue and the carbon side chains of S112, D114, and S118. The 4-methoxy group of **3d** formed an additional H-bond with S118, which is at the bottom of the S3 pocket, and it contributes to the further stabilization of the inhibitor/proteasome complex. These results are in agreement with the SAR data, which show that chain elongation from one to two methylene units favors the proper orientation of the phenylamino moieties in the S3 pocket, and this causes a remarkable increase in the inhibitory activity (compare compounds **3b**, **3c**, and **3d** versus **1e**, **2a**, and **2b** in Table 1).

To better correlate the structures of the complexes of **3c**, **3d**, and **4a** with yeast proteasome to our findings on the inhibition of these compounds towards human proteasome, a superposition of both bovine and mouse constitutive proteasome[1,30] with all three yeast docking complexes was performed. Structures of bovine and mouse proteasomes were used because they are the only two available structures of mammalian constitutive proteasomes. Human proteasome subunits β5 and β6, which form the ChT-L site, are 94–100% identical to their bovine and mouse counterparts. In yeast subunits, only 45–67% of the residues are identical. The overlay revealed a similar conformation of the side chains but with some important differences, most of which were found in the S3 pocket of the ChT-L site. Some of the more notable are the replacement of E120, E122, R125, and H98 in the β6 subunit of yeast proteasome (Figure 4d) with Q120, D122, K125, and Y98 in bovine/mouse/human constitutive proteasome. These changes, which lead to a more spacious S3 pocket in constitutive mouse, bovine, and human proteasomes, rationalize the observed high affinity of **3c**, **3d**, and **4a** for the human particles.

As depicted in Figure 5, inhibitor **5h** bound to the ChT-L active site exhibited an identical positioning of the amide scaffold with an extended conformation and maintaining each amino acid side chain in the same binding pockets as for bortezomib.[13] The ligand did not interact with the active-site β5-T1O$^{\gamma}$ nucleophile, which until now has been considered a common principle of proteasome inhibitor binding. Instead, the amide group was stabilized by H-bonds with β5-T21NH and β5-G47CO main-chain atoms. Additional H-bonds were observed between the pyridinone C=O oxygen atom of **5h** and both β5 A49NH and β6 D114O$^{\gamma}$, this latter through an intervening water molecule located crystallographically in the bortezomib structure and included in our model. Moreover, the phenylamino NH group made a direct H-bond to the protonated D114 residue in the β6 subunit. The isopentyl group of **5h** protruded into the S1 pocket, and made weak hydrophobic contacts with V31, K33, M45, and A49, whereas the (*S*)-benzyl side chain was pointing into the open S2 binding pocket. Finally, the phenylamino substituent was inserted deeply into the S3 pocket and it plays a major role in the differing $K_i$ values amongst the ChT-L, T-L, and PGPH activities.

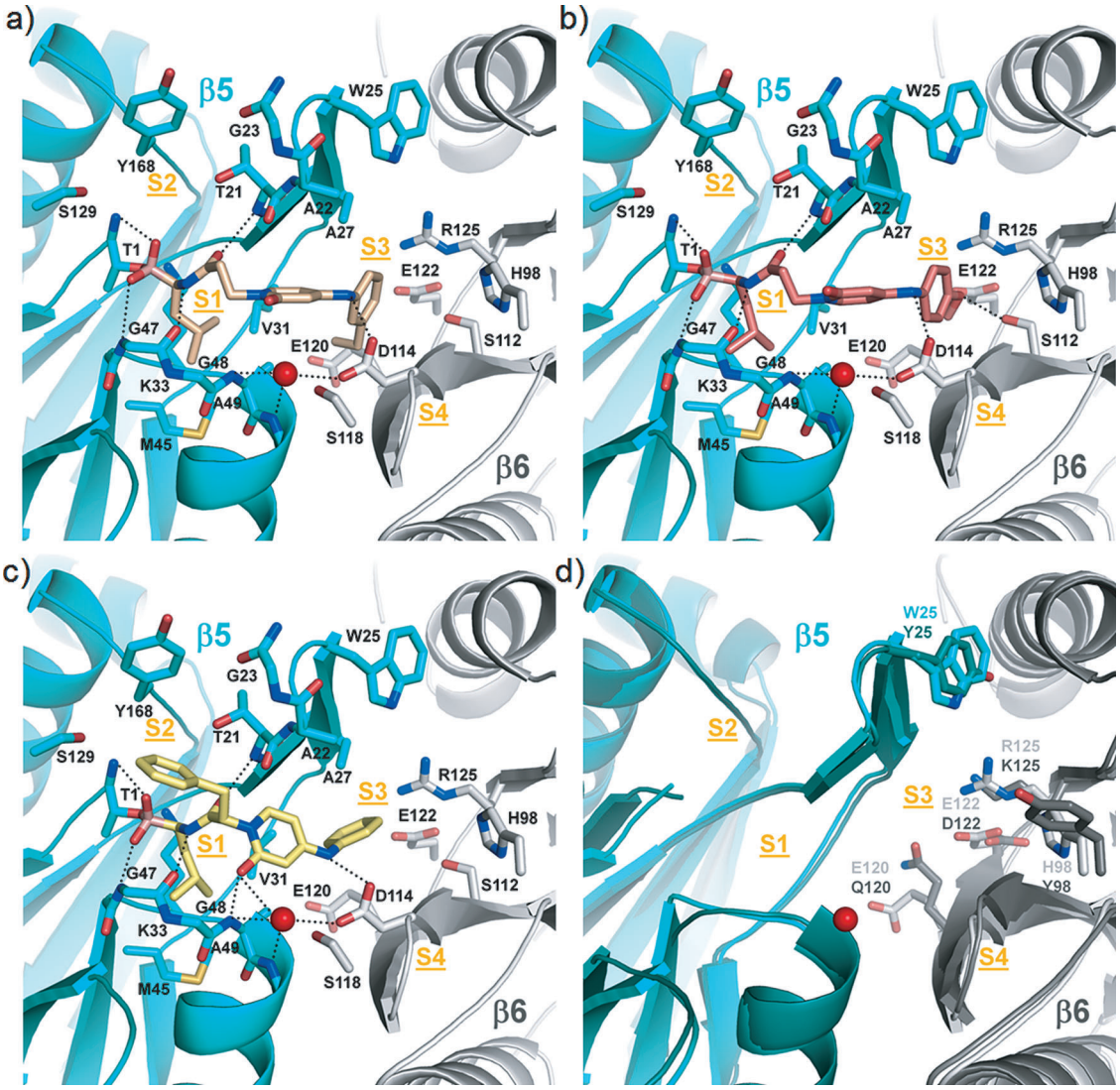


**Figure 4.** Binding modes of compounds a) **3c** (bright orange), b) **3d** (deep salmon), and c) **4a** (yellow) in the β5 (cyan)/β6 (white) active site of yeast 20S proteasome depicted in cartoon form. Only amino acids located within 4 Å of the bound ligand are displayed and labeled. Key H-bonds between the inhibitors and the protein are shown as dashed black lines. The defined water molecule forming tight H-bonds to the protein is displayed as a red sphere. S1–S4 pockets of the proteasome are labeled. d) Close-up view of the S3 pocket in the ChT-L sites of the yeast proteasome superposed with the murine 20S structure highlighted by more discrete colors. Differences in amino acids involved in the substrate binding are highlighted as stick models. According to Schechter nomenclature, the cleavage point is between subsite S1′ and subsite S1 and between the corresponding amino acids P1′ and P1 of the peptide substrate. The $S_1$, $S_2$, $S_3$, and $S_n$ subsites are the residues toward the N-terminus, whereas the $S_1'$, $S_2'$, $S_3'$, and $S_n$ subsites are the ones from the cleavage point toward the C-terminus of the enzyme.

### Determination of the in vitro growth inhibitory activity in the NCI 60 cancer cell line panel

The evaluation of the cytotoxic and/or growth inhibitory effects of both boronates and amides was performed at the NCI. Boronates **1**, **3c**, **3d**, and **4a** and amides **5a** and **5f** were selected for primary screening (one-dose screen). Each compound was evaluated at 10 μM against 60 human tumor cell lines derived from 9 neoplastic diseases: leukemia (L, 6 cell lines), non-small cell lung cancer (NSCLC, 9 cell lines), colon cancer (CC, 7 cell lines), central nervous system cancer (CNSC, 6 cell lines), melanoma (M, 9 cell lines), ovarian cancer (OC, 7 cell lines), renal cancer (RC, 8 cell lines), prostate cancer (PC, 2 cell lines), and breast cancer (BC, 6 cell lines).[31,32]

The obtained results, expressed as % growth mean values against each subpanel, are reported in Table 3. Within the one dose screen, compounds **3d**, **5a**, and **5f** were essentially inactive, whereas remarkable low growth percent values were obtained for **1**, **3c**, and **4a**.

Compounds **1** and **3c** were approved for the further screening test (five-dose screen) at 10-fold dilutions of 5 different concentrations (from 100 to 0.01 μM) on the 60 human tumor cell lines. The antitumor activity of the test compound against each of the 60 cell lines is expressed by three different dose–response parameters: $GI_{50}$ (drug concentration required for 50% growth inhibition), TGI (drug concentration resulting in total growth inhibition), and $LC_{50}$ (drug concentration required for 50% cell death).[32]

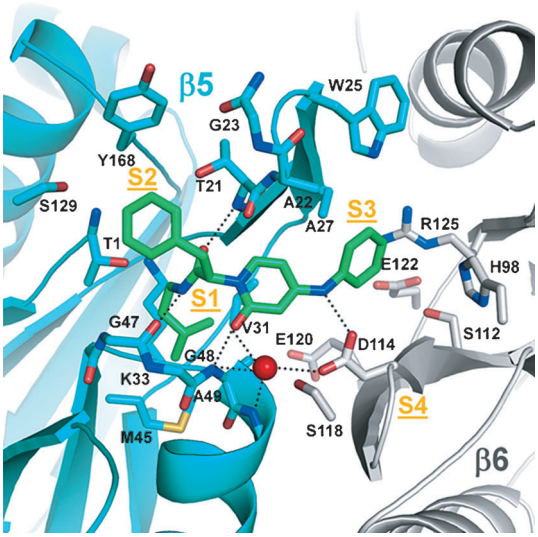


**Figure 5.** Binding mode of non-boronate **5h** (green) into the β5 (cyan)/β6 (white) active site of yeast 20S proteasome depicted in cartoon form. Only amino acids located within 4 Å of the bound ligand are displayed and labeled. Key H-bonds between the inhibitors and the protein are shown as dashed black lines. The defined water molecule forming tight H-bonds to the protein is displayed as a red sphere. S1–S4 pockets of the proteasome are labeled.

**Table 3.** Anticancer activity of lead compound **1**, compounds **3c**, **3d**, **4a**, **5a**, and **5f** as % growth at $10^{-5}$ M.

| Panel/cell line | 1 | 3c | 3d | 4a | 5a | 5f |
|---|---|---|---|---|---|---|
| L | 8.78 | −4.66 | 97.36 | −2.24 | 108.39 | 80.00 |
| NSCLC | 29.99 | 1.43 | 103.34 | −12.87 | 97.21 | 93.51 |
| CC | 24.00 | 8.11 | 105.59 | −22.66 | 103.20 | 102.65 |
| CNSC | 38.03 | 1.99 | 101.14 | −10.79 | 97.03 | 97.7 |
| M | −2.98 | −19.09 | 94.36 | −35.87 | 104.41 | 76.06 |
| OC | 43.81 | 42.77 | 104.01 | 11.87 | 103.29 | 98.01 |
| RC | 23.17 | 15.07 | 101.93 | −22.65 | 92.46 | 93.02 |
| PC | 48.87 | 39.44 | 109.81 | 28.24 | 101.77 | 99.94 |
| BC | 22.15 | 5.01 | 98.52 | −4.43 | 103.55 | 77.59 |

The $GI_{50}$, TGI, and $LC_{50}$ values against the 60 human tumor cell lines for **1** and **3c** are reported in Table 4 and are compared with those of bortezomib (data from NCI). With regard to compound **1**, most of the cell lines were sensitive to this inhibitor and the $GI_{50}$ values were in the micromolar/sub-micromolar range.

Furthermore, compound **1** showed discreet $GI_{50}$ and TGI values on several cell lines: leukemia (MOLT-4, RPMI-8226), non-small cell lung cancer (NCI-H226, NCI-H522), colon cancer (HCT-116), central nervous system cancer (SF-539), melanoma (LOX IMVI, MDA-MB-435, SK-MEL-28, SK-MEL-5), ovarian cancer (OVCAR-3), and breast cancer (MDA-MB-468). Moreover, significant $LC_{50}$ values were obtained on some cell lines such as NCI-H226, LOX IMVI, and MDA-MB-435 belonging to non-small cell lung cancer and melanoma.

Concerning the newly synthesized boronates, inhibitor **3c** showed $GI_{50}$ values at the sub-micromolar level on all the cell lines with the exception of A549/ATCC, HOP-62, NCI-H460, HTC-15, IGROV1, OVCAR-5, OVCAR-8, NCI/ADR-RES, 786-0, and PC-3 (micromolar $GI_{50}$ values). Furthermore, compound **3c** showed good $GI_{50}$ and TGI values on several cell lines, mainly on NCI-H226 (non-small cell lung cancer), SF-539 (CNS cancer), LOX-IMVI (melanoma), MDA-MB-435 (melanoma), HS-587T (breast cancer), and MDA-MB-488 (breast cancer). Moreover, similarly to compound **1**, inhibitor **3c** showed significant $LC_{50}$ values on some cell lines such as NCI-H226 and MDA-MB-435. Dose–response curves of **1** and **3c** against non-small cell lung cancer and melanoma cell lines are reported in Figure 6.

## Conclusions

We developed a series of novel peptidomimetic boronates **2**–**4** structurally related to bortezomib. The synthesized compounds showed a promising inhibitory profile against ChT-L activity with $K_i$ values in the micromolar/nanomolar range; the most active compounds bear a β-alanine or a phenylalanine residue at the P2 site, whereas the presence of a amino group at the 4-position of the pyridone ring enhances the inhibitory properties in view of previously demonstrated ability to establish a H-bond with the side chain of D114 of the β6 subunit.[6] The inhibitors were also proven to co-inhibit the β5 and β1 proteasome subunits, essential for an appropriate antitumor response, and to possess a strong selectivity towards the target enzyme, as no inhibition was recorded against bovine pancreatic α-chymotrypsin.

Docking experiments of the most active inhibitors **3c**, **3d**, **4a**, and **5h** revealed their covalent and noncovalent binding modes and allows future optimization of this interesting class of 20S proteasome inhibitors for cancer treatment. Potent compound **3c** demonstrated efficacy in cellular assays and showed antiproliferative activity at sub-micromolar concentrations.

## Experimental Section

### *Chemistry*

**General**: All reagents and solvents were obtained from commercial suppliers and were used without further purification. Reactions under microwave irradiation were performed with a CEM Discover apparatus. Elemental analyses were performed with a C. Erba Model 1106 (elemental analyzer for C, H, and N), and the obtained results were within ±0.4% of the theoretical values. Merck Silica Gel 60 $F_{254}$ plates were used as analytical TLC; flash column chromatography was performed on Merck Silica Gel (200–400 mesh). $^1$H NMR and $^{13}$C NMR spectra were recorded with Varian Mercury 300 MHz and Bruker 300 MHz spectrometers by using the residual signal of the deuterated solvent as an internal standard. Splitting patterns are described as singlet (s), doublet (d), doublet of doublet (dd), triplet (t), quartet (q), multiplet (m), and broad singlet (br. s). Optical data were detected by a Model 341 PerkinElmer polarimeter.

Compounds **8**, **11a**, **11b**,[6] **11f**, and **11g**,[24] were synthesized as reported in the literature.

**2-(Benzyloxy)-3-bromopyridine (9)**: At 0 °C under an atmosphere of $N_2$, a suspension of KH (333 mg, 8.32 mmol) in dry THF (80 mL)

**Table 4.** In vitro anticancer activity of lead compound **1**, **3c**, and bortezomib against 60 human cancer cell lines.

| Panel/Cell line | Compd **1** | | | Compd **3c** | | | Bortezomib |
|---|---|---|---|---|---|---|---|
| | $GI_{50}$ [μM] | TGI [μM] | $LC_{50}$ [μM] | $GI_{50}$ [μM] | TGI [μM] | $LC_{50}$ [μM] | $GI_{50}$ [nM] |
| *Leukemia* | | | | | | | |
| HL-60(TB) | 3.32 | 72.6 | >100 | 0.31 | 4.03 | >100 | 1.90 |
| K-562 | 3.67 | >100 | >100 | 0.77 | >100 | >100 | 1.17 |
| MOLT-4 | 0.47 | 11.7 | >100 | 0.24 | >100 | >100 | 0.51 |
| RPMI-8226 | 0.34 | 0.95 | >100 | 0.34 | 3.23 | >100 | 0.23 |
| SR | 0.40 | >100 | >100 | 0.25 | – | >100 | 0.85 |
| *Non-small cell lung cancer* | | | | | | | |
| A549/ATCC | 8.34 | >100 | >100 | 4.28 | >100 | >100 | 3.09 |
| HOP-62 | 6.24 | 40.9 | >100 | 2.13 | 8.33 | >100 | 4.47 |
| HOP-92 | 2.49 | 8.23 | 71.0 | 0.52 | 3.46 | 30.3 | 1.00 |
| NCI-H226 | 0.35 | 1.47 | 6.69 | 0.17 | 0.36 | 0.76 | 0.46 |
| NCI-H23 | 3.45 | >100 | >100 | 1.16 | >100 | >100 | 1.00 |
| NCI-H322M | 25.8 | >100 | >100 | 29.9 | >100 | >100 | 17.8 |
| NCI-H460 | 8.41 | 42.5 | >100 | 2.62 | 14.9 | >100 | 4.47 |
| NCI-H522 | 0.93 | 6.44 | >100 | 0.28 | 1.54 | >100 | 1.44 |
| *Colon cancer* | | | | | | | |
| COLO 205 | 8.25 | >100 | >100 | 1.85 | >100 | >100 | 1.23 |
| HCC-2998 | 2.02 | 4.76 | 14.0 | 1.07 | 2.90 | 7.91 | 0.60 |
| HCT-116 | 0.85 | 5.02 | >100 | 0.33 | 1.88 | 58.0 | 0.60 |
| HCT-15 | 8.66 | >100 | >100 | 5.41 | 49.9 | >100 | 1.51 |
| HT29 | 1.06 | 13.2 | >100 | 0.31 | 11.5 | >100 | 0.95 |
| KM12 | 3.08 | 12.4 | 65.0 | 0.63 | 2.86 | 75.3 | 1.70 |
| SW-620 | 2.00 | 23.9 | >100 | 0.33 | 2.53 | >100 | 0.55 |
| *CNS cancer* | | | | | | | |
| SF-268 | 2.88 | 18.6 | >100 | 0.33 | 1.79 | >100 | 1.17 |
| SF-295 | 3.75 | 40.1 | >100 | 0.53 | 2.92 | 35.7 | 1.70 |
| SF-539 | 0.78 | 5.81 | >100 | 0.10 | 0.37 | >100 | 0.59 |
| SNB-19 | 16.6 | >100 | >100 | 0.42 | >100 | >100 | 2.04 |
| SNB-75 | 4.54 | 25.3 | >100 | 0.34 | 3.00 | >100 | 2.04 |
| U251 | 5.04 | >100 | >100 | 0.45 | 25.5 | >100 | 1.55 |
| *Melanoma* | | | | | | | |
| LOX IMVI | 0.64 | 2.27 | 6.23 | 0.21 | 0.64 | 9.52 | 0.78 |
| MALME-3M | 2.08 | 8.77 | >100 | 0.19 | 5.63 | >100 | 0.45 |
| M14 | 1.74 | 13.7 | >100 | 0.26 | 1.13 | >100 | 0.93 |
| MDA-MB-435 | 0.59 | 2.29 | 6.91 | 0.15 | 0.32 | 0.67 | 0.44 |
| SK-MEL-2 | 1.81 | 21.3 | >100 | 0.31 | 2.67 | >100 | 1.07 |
| SK-MEL-28 | 0.66 | 4.49 | >100 | 0.19 | 4.86 | >100 | 0.46 |
| SK-MEL-5 | 0.62 | 2.88 | 14.7 | 0.19 | 1.03 | 21.8 | 0.68 |
| UACC-257 | 1.30 | 7.68 | >100 | 0.72 | 6.61 | >100 | 0.59 |
| UACC-62 | 2.44 | 18.1 | >100 | 0.37 | 1.98 | 27.0 | 0.91 |
| *Ovarian cancer* | | | | | | | |
| IGROV1 | 6.27 | >100 | >100 | 4.28 | 85.8 | >100 | 2.24 |
| OVCAR-3 | 0.51 | 2.78 | 29.7 | 0.18 | 0.47 | 65.0 | 0.54 |
| OVCAR-4 | 5.68 | >100 | >100 | 0.99 | 59.3 | >100 | 1.95 |
| OVCAR-5 | 6.24 | 90.0 | >100 | 3.94 | 73.4 | >100 | 1.55 |
| OVCAR-8 | 5.47 | >100 | >100 | 3.78 | >100 | >100 | 2.63 |
| NCI/ADR-RES | 65.6 | >100 | >100 | >100 | >100 | >100 | 12.3 |
| SK-OV-3 | 11.5 | >100 | >100 | 0.87 | 63.0 | >100 | 13.8 |
| *Renal cancer* | | | | | | | |
| 786-0 | 5.55 | >100 | >100 | 1.51 | >100 | >100 | 1.44 |
| A498 | 1.07 | 6.78 | >100 | 0.20 | 0.77 | >100 | 0.48 |
| ACHN | 3.04 | >100 | >100 | 0.70 | >100 | >100 | 0.79 |
| CAKI-1 | 4.02 | 60.3 | >100 | 4.10 | 31.4 | >100 | 0.66 |
| RXF 393 | 1.81 | 4.78 | 18.1 | 0.35 | 1.59 | 7.74 | 0.71 |
| SN12C | 5.17 | 28.0 | >100 | 0.71 | 6.80 | >100 | 1.10 |
| TK-10 | 3.28 | 25.3 | >100 | 0.66 | 8.20 | >100 | 1.00 |
| UO-31 | 5.59 | 39.6 | >100 | 3.26 | 20.0 | >100 | 1.05 |

was treated with benzyl alcohol (514 μL, 4.99 mmol). After 1 h, a solution of 3-bromo-2-chloropyridine (**7**; 800 mg, 4.16 mmol) in dry THF (5 mL) was added. The mixture was stirred at RT for 18 h. The reaction was quenched with saturated $NH_4Cl$ (20 mL) and THF was removed in vacuo. The product was extracted from the residual aqueous layer with $CH_2Cl_2$ (3×50 mL), and the combined organic phase was dried with $Na_2SO_4$, filtered, and concentrated in vacuo. The crude product was purified by column chromatography (light petroleum/$Et_2O$ 8:2) to yield **9** as a pale yellow oil (1.05 g, 96%). $R_f$=0.74 ($CHCl_3$). $^1$H NMR (300 MHz, $CDCl_3$): $\delta$=5.42 (s, 2H), 6.82–6.92 (m, 2H), 7.32–7.62 (m, 5H), 8.21 ppm (d, $J$=5.3 Hz, 1H).

**2-(Benzyloxy)-*N*-(3-ethylphenyl)pyridin-4-amine (10c)**: Compound **8** (400 mg, 1.82 mmol) was treated with $Pd_2(dba)_3$ (1 mol%), DavePhos (1.5 mol%), 3-ethylaniline (271 μL, 2.18 mmol), *t*BuONa (245 mg, 2.55 mmol), and toluene (4 mL). The mixture was degassed with $N_2$ over 5 min and heated under microwave irradiation at 120–150 °C for 15 min. The suspension was taken up into EtOAc (100 mL), filtered through a short pad of Celite, and concentrated in vacuo. The crude product was purified by column chromatography ($CHCl_3$) to give **10c** (460 mg, 83%) as a yellow oil. $R_f$=0.19 ($CHCl_3$). $^1$H NMR (300 MHz, $CDCl_3$): $\delta$=1.25 (t, $J$=7.0 Hz, 3H), 2.64 (q, $J$=7.62 Hz, 2H), 5.34 (s, 2H), 5.99 (br.s, 1H), 6.33 (d, $J$=1.8 Hz, 1H), 6.47 (dd, $J$=7.62, 1.76 Hz, 1H), 6.94–7.02 (m, 3H), 7.22–7.46 (m, 6H), 7.91 ppm (d, $J$=5.9 Hz, 1H).

**2-(Benzyloxy)-*N*-(4-methoxyphenyl)pyridin-4-amine (10d)**: According to the procedure outlined for **10c**, compound **8** (400 mg, 1.82 mmol) was treated with 4-methoxyaniline (269 mg, 2.18 mmol). Compound **10d** was obtained as a yellow oil (496 mg, 89%) after purification by column chromatography ($CHCl_3$/$CH_3OH$ 9:1). $R_f$=0.64 ($CHCl_3$/$CH_3OH$ 9:1). $^1$H NMR (300 MHz, $CDCl_3$): $\delta$=3.79 (s, 3H), 5.34 (s, 2H), 6.19 (d, $J$=1.8 Hz, 1H), 6.29 (br.s, 1H), 6.35 (dd, $J$=5.9, 1.8 Hz, 1H), 6.88 (d, $J$=8.8 Hz, 2H), 7.1 (d, $J$=8.8 Hz, 2H) 7.25–7.44 (m, 5H), 7.87 ppm (d, $J$=5.9 Hz, 1H).

***N*-Benzyl-2-(benzyloxy)pyridin-4-amine (10e)**: According to the procedure outlined for **10c**, compound **8** (400 mg, 1.82 mmol) was treated with benzylamine (198 μL, 2.18 mmol). Compound **10d** was obtained as a yellow oil (464 mg, 88%) after purification by column chromatography (light petroleum/EtOAc 1:1). $R_f$=0.64 (light petroleum/EtOAc 1:1). $^1$H NMR (300 MHz, $CDCl_3$): $\delta$=4.33 (d, $J$=5.2 Hz, 2H), 5.33 (s, 2H), 5.97 (d, $J$=1.8 Hz, 1H), 6.21 (dd, $J$=5.9, 2.3 Hz, 1H), 7.27–7.46 (m, 10H), 7.83 ppm (d, $J$=5.9 Hz, 1H).

**2-(Benzyloxy)-*N*-phenylpyridin-3-amine (10h)**: According to the procedure outlined for **10c**, compound **9** (500 mg, 1.89 mmol) was treated with aniline (207 μL, 2.27 mmol) and BINAP (1.5 mmol%) in place of the Davephos ligand. Compound **10h** was obtained as a yellow oil (486 mg, 93%) after purification by column chromatography ($CHCl_3$). $R_f$=0.60 ($CHCl_3$). $^1$H NMR (300 MHz, $CDCl_3$): $\delta$=5.50 (s, 2H), 6.17 (br.s, 1H), 6.82–6.86 (m, 1H), 7.03 (t, 1H, $J$=7.6 Hz), 7.15–7.53 (m, 10H), 7.7 ppm (d, 1H, $J$=5.3 Hz).

**Table 4.** (Continued)

| Panel/Cell line | Compd **1** | | | Compd **3c** | | | Bortezomib |
|---|---|---|---|---|---|---|---|
| | $GI_{50}$ [μM] | TGI [μM] | $LC_{50}$ [μM] | $GI_{50}$ [μM] | TGI [μM] | $LC_{50}$ [μM] | $GI_{50}$ [nM] |
| *Prostate cancer* | | | | | | | |
| PC-3 | 5.06 | 36.0 | >100 | 3.50 | >100 | >100 | 2.63 |
| DU-145 | 10.7 | >100 | >100 | 0.74 | 53.3 | >100 | 1.70 |
| *Breast cancer* | | | | | | | |
| MCF7 | 0.43 | >100 | >100 | 0.24 | >100 | >100 | 0.55 |
| MDA-MB-231/ ATCC | 3.09 | 15.2 | >100 | 0.95 | 5.88 | 96.7 | 1.26 |
| HS 578T | 1.86 | 7.16 | >100 | 0.28 | 0.87 | >100 | 1.02 |
| BT-549 | 1.19 | 11.7 | >100 | 0.15 | 1.78 | >100 | 0.55 |
| T-47D | 1.01 | 3.38 | 62.4 | 0.37 | 3.90 | >100 | 0.60 |
| MDA-MB-468 | 0.23 | 5.88 | >100 | 0.09 | 0.59 | >100 | 1.48 |

**2-(Benzyloxy)-3-(piperidin-1-yl)pyridine (10i)**: According to the procedure outlined for **10h**, compound **9** (500 mg, 1.89 mmol) was treated with piperidine (224 μL, 2.27 mmol). Compound **10i** was obtained as a yellow oil (451 mg, 89%) after purification by column chromatography (light petroleum/EtOAc 7:3). $R_f$=0.51 (light petroleum/EtOAc 7:3). $^1$H NMR (300 MHz, $CDCl_3$): $\delta$=1.54–1.79 (m, 6H), 3.03–3.07 (m, 4H), 5.49 (s, 2H), 6.83–6.87 (m, 1H), 7.12 (dd, $J$=7.5, 1.8 Hz, 1H), 7.27–7.54 (m, 5H), 7.80 ppm (dd, $J$=4.8, 1.8 Hz, 1H).

**4-(3-Ethylphenylamino)pyridin-2(1*H*)-one (11c)**: A solution of **10e** (460 mg, 1.51 mmol) in MeOH/EtOAc (2:1, 30 mL) at RT was treated with 10% Pd/C (10 mol%) and fluxed with $H_2$. After 2 h under stirring, the mixture was filtered through a short pad of Celite and washed with EtOAc (150 mL). The solvent was removed in vacuo, and the resulting residue was taken up into $Et_2O$ (15 mL) and filtered to provide **11c** as a white powder (320 mg, 99%). $R_f$=0.19 ($CHCl_3$/MeOH 9:1). $^1$H NMR (300 MHz, $CD_3OD$): $\delta$=1.22 (t, $J$=7.0 Hz, 3H), 2.62 (q, $J$=7.0 Hz, 4H), 5.90 (s, 1H), 6.11 (d, $J$=6.5 Hz, 1H), 6.96–7.28 ppm (m, 5H).

**4-(4-Methoxyphenylamino)pyridin-2(1*H*)-one (11d)**: Starting from **10d** (496 mg, 1.62 mmol), compound **11d** (347 mg, 99%) was obtained according to the procedure outlined for **11c**. $R_f$=0.18 ($CHCl_3$/MeOH 9:1). $^1$H NMR (300 MHz, $CD_3OD$): $\delta$=3.83 (s, 3H), 5.60 (s, 1H), 5.64 (d, $J$=7.9 Hz, 1H), 6.88–7.02 (m, 3H), 7.27 ppm (d, $J$=7.0 Hz, 2H).

**4-(Benzylamino)pyridin-2(1*H*)-one (11e)**: Starting from **10e** (464 mg, 1.60 mmol), compound **11e** (304 mg, 95%) was obtained according to the procedure outlined for **11c**. $R_f$=0.2 ($CHCl_3$/MeOH 9:1). $^1$H NMR (300 MHz, $CD_3OD$): $\delta$=4.32 (s, 2H), 5.40 (d, $J$=1.6 Hz, 1H), 5.96 (dd, $J$=7.0, 2.2 Hz, 1H), 7.10 (d, $J$=7.5 Hz, 1H), 7.20–7.35 ppm (m, 5H).

**3-(Phenylamino)pyridin-2(1*H*)-one (11h)**: Starting from **10h** (486 mg, 1.76 mmol), compound **11h** (317 mg, 97%) was obtained according to the procedure outlined for **11c**. $R_f$=0.38 ($CHCl_3$/MeOH 95:5). $^1$H NMR (300 MHz, $CD_3OD$): $\delta$=6.32 (t, $J$=6.5 Hz, 1H), 6.87 (dd, $J$=6.5, 1.8 Hz, 1H), 6.45–7.0 (m, 1H), 7.17–7.33 ppm (m, 5H).

**3-(Piperidin-1-yl)pyridin-2(1*H*)-one (11i)**: Starting from **10i** (451 mg, 1.68 mmol), compound **11i** (296 mg, 99%) was obtained according to the procedure outlined for **11c**. $R_f$=0.68 ($CHCl_3$/MeOH 9:1). $^1$H NMR (300 MHz, $CD_3OD$): $\delta$=1.58–1.79 (m, 6H), 2.98–3.01 (m, 4H), 6.32 (t, $J$=7.0 Hz, 1H), 6.94 (dd, $J$=7.5, 1.8 Hz, 2H), 7.04 ppm (dd, $J$=6.6, 1.8 Hz, 2H).

**Ethyl 2-[4-(3-ethylphenylamino)-2-oxopyridin-1(2*H*)-yl]acetate (12a)**: A solution of **11c** (160 mg, 0.75 mmol) in dry DMF (10 mL) was treated with NaH (22 mg, 8.96 mmol) at 0 °C. After 1 h, ethyl bromoacetate (83 μL, 0.75 mmol) was added, and the mixture was stirred for 2 h at RT. The mixture was quenched with saturated $NH_4Cl$ (5 mL), and the product was extracted with $CH_2Cl_2$ (3×70 mL). The organic layer was washed with water (3×100 mL), dried with $Na_2SO_4$, filtered, and concentrated in vacuo. The crude product was purified by column chromatography ($CHCl_3$/MeOH 9:1) to give **12a** as a yellow oil (295 mg, 66%). $R_f$=0.43 ($CHCl_3$/MeOH 95:5). $^1$H NMR (300 MHz, $CD_3OD$): $\delta$=1.09–1.21 (m, 6H), 2.47–2.64 (m, 2H), 4.07–4.14 (m, 2H), 4.47 (s, 2H), 5.89–5.92 (m, 2H), 6.83–7.15 ppm (m, 5H).

**Ethyl 2-[4-(4-methoxyphenylamino)-2-oxopyridin-1(2*H*)-yl]acetate (12b)**: Starting from pyridone **11d** (173 mg, 0.80 mmol), compound **12b** (162 mg, 67%) was obtained as a yellow oil according to the procedure outlined for **12a**. $R_f$=0.44 ($CHCl_3$/MeOH 95:5). $^1$H NMR (300 MHz, $CD_3OD$): $\delta$=1.29 (t, $J$=7.9 Hz, 3H), 3.81 (s, 3H), 4.23 (q, $J$=7.0 Hz, 2H), 4.69 (s, 2H), 5.79–5.84 (m, 2H), 6.03–6.13 (m, 1H), 6.87–7.13 ppm (m, 4H).

**Ethyl 2-[4-(benzylamino)-2-oxopyridin-1(2*H*)-yl]acetate (12c)**: Starting from pyridone **11e** (304 mg, 1.52 mmol), compound **12c** (305 mg, 70%) was obtained as a yellow oil according to the procedure outlined for **12a**. $R_f$=0.28 ($CHCl_3$/MeOH 95:5). $^1$H NMR (300 MHz, $CD_3OD$): $\delta$=1.25 (t, $J$=7.0 Hz, 3H), 4.18 (q, $J$=7.0 Hz, 2H), 4.31 (s, 2H), 4.54 (s, 2H), 5.43 (d, $J$=2.3 Hz, 1H), 5.98 (dd, $J$=7.6, 2.9 Hz, 1H), 7.22–7.33 ppm (m, 6H).

**Ethyl 2-[2-oxo-3-(phenylamino)pyridin-1(2*H*)-yl]acetate (12d)**: Starting from pyridone **11h** (158 mg, 0.85 mmol), compound **12d** (178 mg, 77%) was obtained as a yellow oil according to the procedure outlined for **12a**. $R_f$=0. 67 ($CHCl_3$/MeOH 95:5). $^1$H NMR (300 MHz, $CDCl_3$): $\delta$=1.29 (t, $J$=7.3 Hz, 3H), 4.25 (q, $J$=7.3 Hz, 2H), 4.68 (s, 2H), 6.17 (t, $J$=6.9 Hz, 1H), 6.70 (d, $J$=6.9 Hz, 1H), 6.96–7.33 ppm (m, 6H).

**Ethyl 2-[2-oxo-3-(piperidin-1-yl)pyridin-1(2*H*)-yl]acetate (12e)**: Starting from pyridone **11i** (296 mg, 1.66 mmol), compound **12e** (285 mg, 65%) was obtained as a yellow oil according to the procedure outlined for **12a**. $R_f$=0.48 ($CHCl_3$/MeOH 98:2). $^1$H NMR (300 MHz, $CDCl_3$): $\delta$=1.27 (t, $J$=7.3 Hz, 3H), 1.55–1.72 (m, 6H), 3.03 (s, 4H), 4.22 (q, $J$=7.6 Hz, 2H), 4.59 (s, 2H), 6.11–6.16 (m, 1H), 6.65 (d, $J$=7.0 Hz, 1H), 6.87 ppm (d, $J$=6.5 Hz, 1H).

**Methyl 3-[2-oxopyridin-1(2*H*)-yl]propanoate (12f)**: According to the procedure outlined for **12a**, compound **11a** (300 mg, 3.15 mmol) was treated with methyl 3-bromoproprionate (481 μL, 4.41 mmol). Compound **12f** was obtained as a yellow oil (474 mg, 83%) after purification by column chromatography ($CHCl_3$/MeOH 95:5). $R_f$=0.70 ($CHCl_3$/MeOH 95:5). $^1$H NMR (300 MHz, $CDCl_3$): $\delta$=2.33 (t, $J$=6.5 Hz, 2H), 3.13 (s, 3H), 3.69 (t, $J$=7.0 Hz, 2H), 5.67 (t, $J$=7.0 Hz, 1H), 5.98 (d, $J$=8.8 Hz, 1H), 6.82–6.88 (m, 1H), 7.05 ppm (dd, $J$=6.5, 1.8 Hz, 1H).

**Methyl 3-[2-oxo-4-(phenylamino)pyridin-1(2*H*)-yl]propanoate (12g)**: A solution of **11b** (300 mg, 1.61 mmol) in dry DMF (10 mL) was treated with NaH (46 mg, 1.93 mmol) at 0 °C. After 1 h, methyl 3-bromopropionate (246 μL, 2.54 mmol) was added, and the mixture was heated at reflux for 12 h. The mixture was quenched with saturated $NH_4Cl$ (5 mL), and the product was extracted with $CH_2Cl_2$

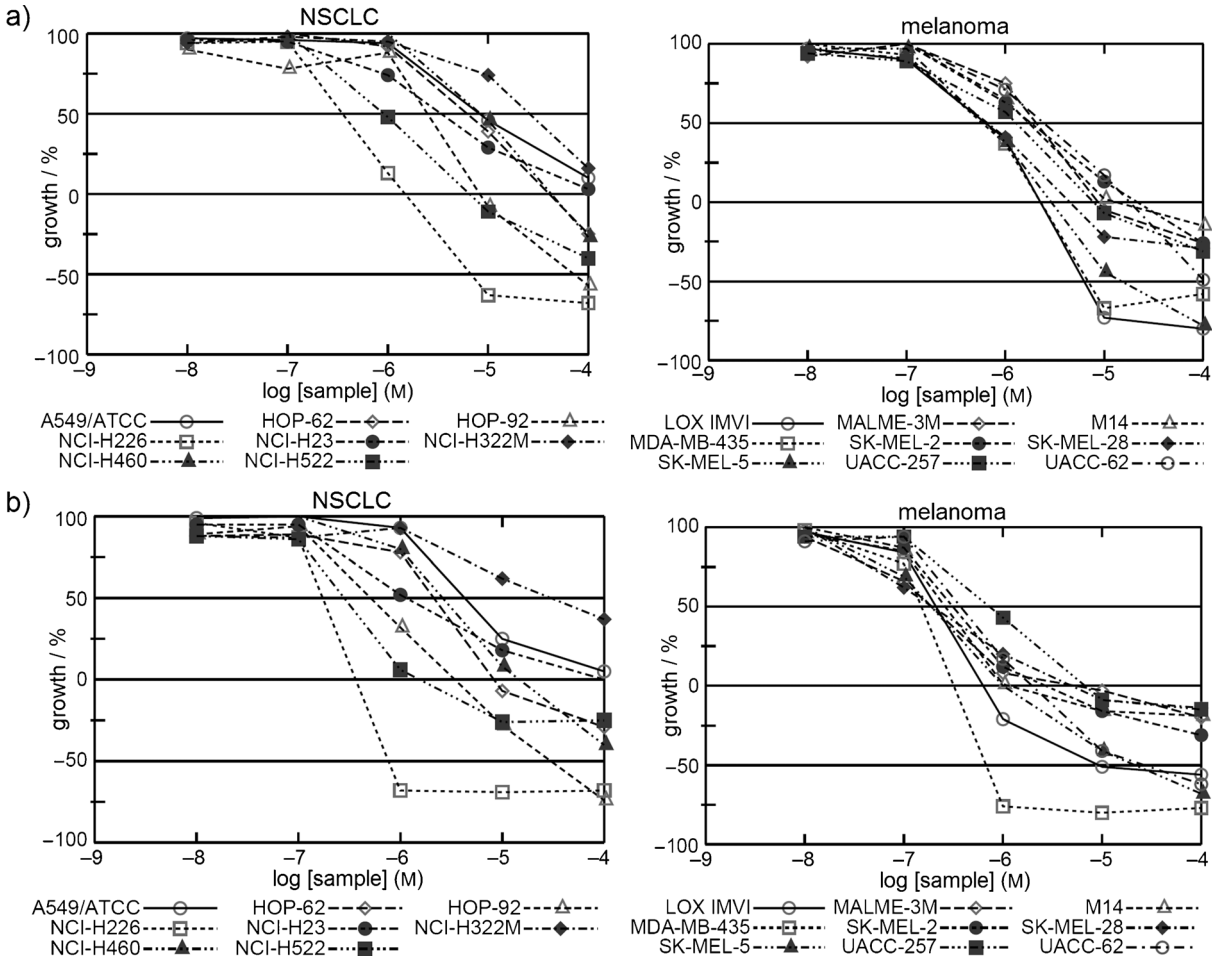


**Figure 6.** Dose–response curves of a) **1** and b) **3c** against non-small cell lung cancer (NSCLC) and melanoma cell lines.

(3×70 mL). The organic layer was washed with water (3×100 mL), dried with $Na_2SO_4$, filtered, and concentrated in vacuo. The crude product was purified by column chromatography ($CHCl_3$/MeOH 95:5) to give **12g** as a yellow oil (263 mg, 60%). $R_f$=0.34 ($CHCl_3$/MeOH 95:5). $^1$H NMR (300 MHz, $CDCl_3$): $\delta$=2.55 (t, $J$=7.0 Hz, 2H), 3.57 (s, 3H), 3.88 (t, $J$=7.0 Hz, 2H), 5.73 (d, $J$=2.2 Hz, 1H), 6.00 (dd, $J$=7.5, 2.2 Hz, 1H), 7.01 (t, $J$=7.5 Hz, 1H), 7.15–7.40 ppm (m, 5H).

**Methyl 3-[4-(3-ethylphenylamino)-2-oxopyridin-1(2*H*)-yl]propanoate (12h)**: Starting from pyridone **11c** (160 mg, 0.75 mmol), compound **12h** (130 mg, 58%) was obtained as a yellow oil according to the procedure outlined for **12g**. $R_f$=0.40 ($CHCl_3$/MeOH 95:5). $^1$H NMR (300 MHz, $CDCl_3$) $\delta$=1.13 (t, $J$=7.5 Hz, 3H), 2.52 (q, $J$=7.5 Hz, 2H), 2.74 (t, $J$=6.2 Hz, 2H), 3.59 (s, 3H), 4.02 (t, $J$=6.2 Hz, 2H), 5.91 (dd, $J$=7.5, 2.2 Hz, 1H), 5.96 (d, $J$=2.6 Hz, 1H), 6.84–7.15 (m, 5H), 7.43 ppm (s, 1H).

**Methyl 3-[4-(4-methoxyphenylamino)-2-oxopyridin-1(2*H*)-yl]propanoate (12i)**: Starting from pyridone **11d** (173 mg, 0.80 mmol), compound **12i** (145 mg, 60%) was obtained as a yellow oil according to the procedure outlined for **12g**. $R_f$=0.38 ($CHCl_3$/MeOH 95:5). $^1$H NMR (300 MHz, $CDCl_3$): $\delta$=2.82 (t, $J$=6.2 Hz, 2H), 3.67 (s, 3H), 3.80 (s, 3H), 4.08 (t, $J$=6.2 Hz, 2H), 5.72–5.75 (m, 2H), 5.84 (br. s, 1H), 6.84–6.90 (m, 2H), 7.07–7.12 (m, 2H), 7.23 ppm (d, $J$=7.0 Hz, 1H).

**Methyl 3-[2-oxo-4-(piperidin-1-yl)pyridin-1(2*H*)-yl]propanoate (12j)**: Starting from pyridone **11f** (300 mg, 1.68 mmol), compound **12j** (275 mg, 62%) was obtained as a yellow oil according to the procedure outlined for **12g**. $R_f$=0.45 ($CHCl_3$/MeOH 95:5). $^1$H NMR (300 MHz, $CDCl_3$): $\delta$=1.50 (s, 6H), 2.69–2.73 (m, 2H), 2.85–3.16 (m, 4H), 3.54 (s, 3H), 3.95–3.98 (m, 2H), 5.57 (s, 1H), 5.79 (d, $J$=7.6 Hz, 1H), 7.10 ppm (d, $J$=7.6 Hz, 1H).

**Methyl 3-[4-(4-methylpiperazin-1-yl)-2-oxopyridin-1(2*H*)-yl]propanoate (12k)**: Starting from pyridone **11g** (300 mg, 1.55 mmol), compound **12k** (238 mg, 55%) was obtained as a yellow oil according to the procedure outlined for **12g**. $R_f$=0. 37 ($CHCl_3$/MeOH 95:5). $^1$H NMR (300 MHz, $CDCl_3$): $\delta$=2.32 (s, 3H), 2.53 (t, $J$=5.3 Hz, 4H), 2.79 (t, $J$=6.5 Hz, 2H), 3.31 (t, $J$=5.3 Hz, 2H), 3.63 (s, 3H), 4.06 (t, $J$=6.5 Hz, 2H), 5.76 (d, $J$=2.9 Hz, 1H), 5.88 (dd, $J$=7.6, 2.9 Hz, 1H), 7.24 ppm (d, $J$=7.6 Hz, 1H).

**Methyl 3-[2-oxo-3-(phenylamino)pyridin-1(2*H*)-yl]propanoate (12l)**: Starting from pyridone **11h** (158 mg, 0.85 mmol), compound **12l** (163 mg, 71%) was obtained as a yellow oil according to the procedure outlined for **12g**. $R_f$=0.40 ($CHCl_3$/MeOH 95:5). $^1$H NMR (300 MHz, $CDCl_3$): $\delta$=2.90 (t, $J$=6.6 Hz, 2H), 3.69 (s, 3H), 4.27 (t, $J$=6.6 Hz, 2H), 6.14 (t, $J$=7.0 Hz, 1H), 6.89 (dd, $J$=7.0, 1.8 Hz, 1H), 6.98–7.07 (m, 2H), 7.18 (d, $J$=7.5 Hz, 1H), 7.32 ppm (q, $J$=7.5 Hz, 2H).

**(*S*)-Methyl 2-[2-oxo-4-(phenylamino)pyridin-1(2*H*)-yl]-3-phenylpropanoate (12m)**: According to the procedure outlined for **12g**, compound **11b** (300 mg, 1.61 mmol) was treated with (*R*)-methyl 3-phenyl-2-(trifluoromethylsulfonyl)propanoate (603 mg,

1.93 mmol) synthesized as reported in the literature.[5] Compound **12m** was obtained as a yellow oil (280 mg, 50%) after purification by column chromatography (EtOAc/*n*-hexane/*i*PrOH 6:3:1). $R_f$ = 0.58 (EtOAc/*n*-hexane/*i*PrOH 6:3:1). $^1$H NMR (300 MHz, $CD_3OD$): $\delta$ = 3.65 (s, 3H), 4.08–4.15 (m, 1H), 4.38–4.45 (m, 1H), 5.11–5.16 (m, 1H), 5.84–5.92 (m, 2H), 7.00 (d, $J$ = 7.6 Hz, 1H), 7.08–7.38 ppm (m, 10H).

**(*R*)-Methyl 2-[2-oxo-4-(phenylamino)pyridin-1(2*H*)-yl]-3-phenylpropanoate (12n)**: According to the procedure outlined for **12g**, compound **11b** (300 mg, 1.61 mmol) was treated with (*S*)-methyl 3-phenyl-2-(trifluoromethylsulfonyl)propanoate (603 mg, 1.93 mmol) synthesized as reported in the literature.[5] Compound **12n** was obtained as a yellow oil (319 mg, 57%) after purification by column chromatography (EtOAc/*n*-hexane/*i*PrOH 6:3:1). $R_f$ = 0.58 (EtOAc/*n*-hexane/*i*PrOH 6:3:1). $^1$H NMR (300 MHz, $CD_3OD$): $\delta$ = 3.63 (s, 3H), 4.11–4.16 (m, 1H), 4.36–4.44 (m, 1H), 5.17–5.21 (m, 1H), 5.80–5.88 (m, 2H), 7.12 (d, $J$ = 7.0 Hz, 1H), 7.11–7.43 ppm (m, 10H).

**2-[4-(3-Ethylphenylamino)-2-oxopyridin-1(2*H*)-yl]acetic acid (13a)**: 1 N LiOH (1.96 mL) was added at 0 °C to a solution of ester **12a** (295 mg, 0.98 mmol) in EtOH/$H_2O$ (1:1, 30 mL). After 4 h at RT, the organic layer was evaporated in vacuo and the residual aqueous solution was treated with 6 N HCl (pH ≈ 6.8). The mixture was concentrated at reduced pressure, and the residue was purified by column chromatography (3% HCOOH in $CHCl_3$/MeOH 9:1) to give **13a** as a white powder (264 mg, 99%). $R_f$ = 0.24 (3% HCOOH in $CHCl_3$/MeOH 9:1). $^1$H NMR (300 MHz, $CD_3OD$): $\delta$ = 1.20 (t, $J$ = 7.0 Hz, 3H), 2.56 (m, $J$ = 7.0 Hz, 2H), 4.50 (s, 2H), 5.87–5.93 (m, 2H), 6.80–7.11 ppm (m, 5H).

**2-[4-(4-Methoxyphenylamino)-2-oxopyridin-1(2*H*)-yl]acetic acid (13b)**: Compound **13b** (145 mg, 99%) was obtained from ester **13b** (162 mg, 0.54 mmol) according to the procedure outlined for **13a**. $R_f$ = 0.26 (3% HCOOH in $CHCl_3$/MeOH 9:1). $^1$H NMR (300 MHz, $CD_3OD$): $\delta$ = 3.83 (s, 3H), 4.74 (s, 2H), 5.81–5.85 (m, 2H), 6.12–6.20 (m, 1H), 6.94–7.11 ppm (m, 4H).

**2-[4-(Benzylamino)-2-oxopyridin-1(2*H*)-yl]acetic acid (13c)**: Compound **13c** (271 mg, 99%) was obtained from ester **12c** (305 mg, 1.06 mmol) according to the procedure outlined for **13a**. $R_f$ = 0.19 (3% HCOOH in $CHCl_3$/MeOH 9:1). $^1$H NMR (300 MHz, [$D_6$]DMSO): $\delta$ = 4.18 (s, 2H), 4.27 (s, 2H), 5.06 (s, 1H), 5.76–5.79 (m, 1H), 7.20–7.28 ppm (m, 6H).

**2-[2-Oxo-3-(phenylamino)pyridin-1(2*H*)-yl]acetic acid (13d)**: Compound **13d** (153 mg, 97%) was obtained from ester **12d** (178 mg, 0.65 mmol) according to the procedure outlined for **13a**. $R_f$ = 0.25 (3% HCOOH in $CHCl_3$/MeOH 9:1). $^1$H NMR (300 MHz, $CDCl_3$): $\delta$ = 4.67 (s, 2H), 6.27 (t, $J$ = 6.9 Hz, 1H), 6.99 (d, $J$ = 6.9 Hz, 1H), 7.12–7.43 ppm (m, 6H).

**2-[2-Oxo-3-(piperidin-1-yl)pyridin-1(2*H*)-yl]acetic acid (13e)**: Compound **13e** (253 mg, 99%) was obtained from ester **11e** (285 mg, 1.08 mmol) according to the procedure outlined for **13a**. $R_f$ = 0.28 (3% HCOOH in $CHCl_3$/MeOH 9:1). $^1$H NMR (300 MHz, $CD_3OD$): $\delta$ = 1.57–1.71 (m, 6H), 2.95–2.98 (m, 4H), 4.54 (s, 2H), 6.29 (t, $J$ = 6.5 Hz, 1H), 6.91 (d, $J$ = 6.5 Hz, 1H), 7.19 ppm (d, $J$ = 7.0 Hz, 1H).

**3-[2-Oxopyridin-1(2*H*)-yl]propanoic acid (13f)**: At 0 °C, 1 N LiOH (5 mL) was added to a solution of ester **12f** (474 mg, 2.62 mmol) in MeOH/$H_2O$ (1:1, 30 mL). After 4 h at RT, the MeOH was evaporated in vacuo. The residual aqueous solution was treated with 6 N HCl (pH ≈ 3), and the product was extracted with EtOAc (3× 30 mL). The organic layer was dried with $Na_2SO_4$, filtered, and evaporated in vacuo to provide **13f** (416 mg, 95%), which was directly used without further purification. $R_f$ = 0.33 (MeOH). $^1$H NMR (300 MHz, [$D_6$]DMSO): $\delta$ = 1.57–1.71 (m, 6H), 2.95–2.98 (m, 4H), 4.54 (s, 2H), 6.29 (t, $J$ = 6.5 Hz, 1H), 6.91 (d, $J$ = 6.5 Hz, 1H), 7.19 ppm (d, $J$ = 7.0 Hz, 1H).

**3-[2-Oxo-4-(phenylamino)pyridin-1(2*H*)-yl]propanoic acid (13g)**: Starting from a solution of ester **12g** (263 mg, 0.96 mmol) in MeOH/$H_2O$ (1:1, 30 mL), compound **13g** (245 mg, 99%) was obtained according to the procedure outlined for **13a**. $R_f$ = 0.29 (3% HCOOH in $CHCl_3$/MeOH 9:1). $^1$H NMR (300 MHz, [$D_6$]DMSO): $\delta$ = 2.57 (t, $J$ = 6.6 Hz, 2H), 3.89 (t, $J$ = 7.0 Hz, 2H), 5.73 (d, $J$ = 2.2 Hz, 1H), 6.0 (dd, $J$ = 7.5, 2.2 Hz, 1H), 7.02 (t, $J$ = 7.5 Hz, 1H), 7.16 (d, $J$ = 7.5 Hz, 2H), 7.31 (t, $J$ = 7.9 Hz, 2H), 7.42 ppm (d, $J$ = 7.5 Hz, 1H).

**3-[4-(3-Ethylphenylamino)-2-oxopyridin-1(2*H*)-yl]propanoic acid (13h)**: Compound **13h** (123 mg, 98%) was obtained from ester **12h** (130 mg, 0.44 mmol) according to the procedure outlined for **13g**. $R_f$ = 0.31 (3% HCOOH in $CHCl_3$/MeOH 9:1). $^1$H NMR (300 MHz, [$D_6$]DMSO) $\delta$ = 1.11 (t, $J$ = 7.5 Hz, 3H), 2.53 (q, $J$ = 7.5 Hz, 2H), 2.76 (t, $J$ = 6.2 Hz, 2H), 4.15 (t, $J$ = 6.6 Hz, 2H), 6.01 (dd, $J$ = 7.5, 1.8 Hz, 1H), 6.66 (d, $J$ = 1.8 Hz, 1H), 6.91–7.23 ppm (m, 6H).

**3-[4-(4-Methoxyphenylamino)-2-oxopyridin-1(2*H*)-yl]propanoic acid (13i)**: Compound **13i** (137 mg, 99%) was obtained from ester **12i** (145 mg, 0.48 mmol) according to the procedure outlined for **13g**. $R_f$ = 0.31 (3% HCOOH in $CHCl_3$/MeOH 9:1). $^1$H NMR (300 MHz, [$D_6$]DMSO): $\delta$ = 2.94 (t, $J$ = 6.3 Hz, 2H), 3.76 (s, 3H), 4.16 (t, $J$ = 6.3 Hz, 2H), 5.88–5.97 (m, 2H), 6.90–7.21 ppm (m, 5H).

**3-[2-Oxo-4-(piperidin-1-yl)pyridin-1(2*H*)-yl]propanoic acid (13j)**: Compound **13j** (248 mg, 95%) was obtained from ester **12j** (275 mg, 1.04 mmol) according to the procedure outlined for **13g**. $R_f$ = 0.33 (3% HCOOH in $CHCl_3$/MeOH 9:1). $^1$H NMR (300 MHz, [$D_6$]DMSO): $\delta$ = 1.43 (s, 6H), 2.70 (t, $J$ = 6.3 Hz, 2H), 2.83–3.11 (m, 4H), 3.93 (t, $J$ = 6.3 Hz, 2H), 5.79 (s, 1H), 6.03 (dd, $J$ = 7.6, 1.8 Hz, 1H), 7.22 ppm (d, $J$ = 7.6 Hz, 1H).

**3-[4-(4-Methylpiperazin-1-yl)-2-oxopyridin-1(2*H*)-yl]propanoic acid (13k)**: Compound **13k** (220 mg, 97%) was obtained from ester **12k** (238 mg, 0.85 mmol) according to the procedure outlined for **13g**. $R_f$ = 0.23 (3% HCOOH in $CHCl_3$/MeOH 9:1). $^1$H NMR (300 MHz, [$D_6$]DMSO): $\delta$ = 2.30 (s, 3H), 2.55 (t, $J$ = 5.3 Hz, 4H), 2.88 (t, $J$ = 6.5 Hz, 2H), 3.33 (t, $J$ = 5.3 Hz, 2H), 4.13 (t, $J$ = 6.5 Hz, 2H), 5.88 (d, $J$ = 2.2 Hz, 1H), 6.03 (dd, $J$ = 7.0, 2.2 Hz, 1H), 7.27 ppm (d, $J$ = 7.0 Hz, 1H).

**3-[2-Oxo-3-(phenylamino)pyridin-1(2*H*)-yl]propanoic acid (13l)**: Compound **13l** (152 mg, 99%) was obtained from ester **12l** (163 mg, 0.60 mmol) according to the procedure outlined for **13g**. $R_f$ = 0.31 (3% HCOOH in $CHCl_3$/MeOH 9:1). $^1$H NMR (300 MHz, [$D_6$]DMSO): $\delta$ = 3.11 (t, $J$ = 6.6 Hz, 2H), 4.20 (t, $J$ = 6.6 Hz, 2H), 6.23 (t, $J$ = 7.0 Hz, 1H), 6.95 (dd, $J$ = 7.0, 1.6 Hz, 1H), 7.13–7.38 ppm (m, 5H).

**(*S*)-2-[2-Oxo-4-(phenylamino)pyridin-1(2*H*)-yl]-3-phenylpropanoic acid (13m)**: Compound **13m** (259 mg, 97%) was obtained from ester **12m** (280 mg, 0.80 mmol) according to the procedure outlined for **13g**. $R_f$ = 0.15 (3% HCOOH in $CHCl_3$/MeOH 9:1). $[\alpha]_D^{20}$ = −26.8 ($c$ = 0.5, DMSO). $^1$H NMR (300 MHz, $CD_3OD$): $\delta$ = 3.47–3.55 (m, 1H), 3.99–4.06 (m, 1H), 5.49–5.56 (m, 1H), 5.86–6.08 (m, 2H), 7.07–7.33 ppm (m, 11H). .

**(*R*)-2-[2-Oxo-4-(phenylamino)pyridin-1(2*H*)-yl]-3-phenylpropanoic acid (13n)**: Compound **13n** (304 mg, 99%) was obtained from ester **12n** (319 mg, 0.91 mmol) according to the procedure outlined for **13g**. $R_f$ = 0.15 (3% HCOOH in $CHCl_3$/MeOH 9:1). $[\alpha]_D^{20}$ = +

27.1 ($c = 0.5$, DMSO). $^1$H NMR (300 MHz, $CD_3OD$): $\delta = 3.40$–$3.49$ (m, 1H), 3.90–4.01 (m, 1H), 5.55–5.67 (m, 1H), 5.89–6.08 (m, 2H), 7.13–7.31 ppm (m, 11H).

**(*R*)-1-{2-[4-(3-Ethylphenylamino)-2-oxopyridin-1(2*H*)-yl]acetamido}-3-methylbutylboronic acid pinanediol ester (15a)**: A suspension (−5 °C) of acid **13a** (264 mg, 0.97 mmol) in dry $CH_2Cl_2$ (20 mL) was treated with HOBt (315 mg, 2.33 mmol) at −5 °C. After 20 min, the reaction mixture was further cooled to −15 °C and EDC·HCl (446 mg, 2.33 mmol), a precooled (0 °C) solution of commercially available pinanediol L-leucine boronate trifluoroacetate salt (**14**; 368 mg, 0.97 mmol) and DIPEA (202 μL, 1.16 mmol) in dry $CH_2Cl_2$ (5 mL) were added. After 1 h and additional 2 h at RT, the solution was washed in sequence with 0.1 M $KHSO_4$, 5% $NaHCO_3$, and brine, and then dried with $Na_2SO_4$, filtered, and concentrated under reduced pressure. The residue was taken up into $Et_2O$ (20 mL) and filtered. The organic layer was evaporated to give **15a** (403 mg, 80%) as a pale yellow oil, which was directly used in the next step without any further purification. $R_f = 0.72$ ($CHCl_3$/MeOH 9:1).

**(*R*)-1-{2-[4-(4-Methoxyphenylamino)-2-oxopyridin-1(2*H*)-yl]acetamido}-3-methylbutylboronic acid pinanediol ester (15b)**: According to the procedure described for **15a**, **15b** (214 mg, 77%) was obtained from acid **13b** (145 mg, 0.53 mmol). Compound **15b** was directly used in the next step without any further purification. The solid residue, obtained from filtration, was purified by column chromatography ($CHCl_3$/MeOH 95:5) to provide byproduct **5a** (42 mg, 23%) as a white powder. $R_f = 0.58$ ($CHCl_3$/MeOH 95:5).

**(*R*)-1-{2-[4-(Benzylamino)-2-oxopyridin-1(2*H*)-yl]acetamido}-3-methylbutylboronic acid pinanediol ester (15c)**: According to the procedure described for **15a**, compound **15c** (372 mg, 70%) was obtained from acid **13c** (271 mg, 1.05 mmol) and was directly used in the next step without any further purification. $R_f = 0.64$ ($CHCl_3$/MeOH 9:1).

**(*R*)-1-{2-[2-Oxo-3-(phenylamino)pyridin-1(2*H*)-yl]acetamido}-3-methylbutylboronic acid pinanediol ester (15d)**: According to the procedure described for **15b**, compounds **15d** (217 mg, 75%) and **5b** (39 mg, 20%) were obtained from acid **13d** (153 mg, 0.63 mmol). Compound **15d** was directly used in the next step without any further purification. $R_f = 0.83$ ($CHCl_3$/MeOH 9:1).

**(*R*)-1-{2-[2-Oxo-3-(piperidin-1-yl)pyridin-1(2*H*)-yl]acetamido}-3-methylbutylboronic acid pinanediol ester (15e)**: According to the procedure described for **15b**, compounds **15e** (430 mg, 83%) and **5c** (36 mg, 11%) were obtained from acid **13e** (253 mg, 1.07 mmol). Compound **15e** was directly used in the next step without purification. $R_f = 0.22$ ($CHCl_3$/MeOH 95:5).

**(*R*)-1-{3-[2-Oxopyridin-1(2*H*)-yl]propanamido}-3-methylbutylboronic acid pinanediol ester (15f)**: According to the procedure described for **15b**, compounds **15f** (825 mg, 80%) and **5d** (59 mg, 10%) were obtained from acid **13f** (416 mg, 2.49 mmol): Compound **15f** was directly used in the next step without any further purification. $R_f = 0.73$ ($CHCl_3$/MeOH 9:1).

**(*R*)-1-{3-[2-Oxo-4-(phenylamino)pyridin-1(2*H*)-yl]propanamido}-3-methylbutylboronic acid pinanediol ester (15g)**: According to the procedure described for **15b**, compounds **15g** (339 mg, 70%) and **5e** (56 mg, 18%) were obtained from acid **13g** (245 mg, 0.95 mmol). Compound **15g** was directly used in the next step without any further purification. $R_f = 0.56$ ($CHCl_3$/MeOH 9:1).

**(*R*)-1-{3-[4-(3-Ethylphenylamino)-2-oxopyridin-1(2*H*)-yl]propanamido}-3-methylbutylboronic acid pinanediol ester (15h)**: According to the procedure described for **15a**, compound **15h** (187 mg, 82%) was obtained from acid **13h** (123 mg, 0.43 mmol) and was directly used in the next step without any further purification. $R_f = 0.61$ ($CHCl_3$/MeOH 9:1).

**(*R*)-1-{3-[4-(4-Methoxyphenylamino)-2-oxopyridin-1(2*H*)-yl]propanamido}-3-methylbutylboronic acid pinanediol ester (15i)**: According to the procedure described for **15b**, compounds **15i** (206 mg, 80%) and **5f** (34 mg, 20%) were obtained from acid **13i** (137 mg, 0.48 mmol). Compound **15i** was directly used in the next step without any further purification. $R_f = 0.61$ ($CHCl_3$/MeOH 9:1).

**(*R*)-1-{3-[2-Oxo-4-(piperidin-1-yl)pyridin-1(2*H*)-yl]propanoyloxy}-3-methylbutylboronic acid pinanediol ester (15j)**: According to the procedure described for **15b**, compounds **15j** (418 mg, 85%) and **5g** (51 mg, 16%) were obtained from acid **13j** (248 mg, 0.99 mmol). Compound **15j** was directly used in the next step without any further purification. $R_f = 0.57$ ($CHCl_3$/MeOH 9:1).

**(*R*)-1-{3-[4-(4-Methylpiperazin-1-yl)-2-oxopyridin-1(2*H*)-yl]propanamido}-3-methylbutylboronic acid pinanediol ester (15k)**: According to the procedure described for **15a**, compound **15k** (308 mg, 72%) was obtained from acid **13k** (220 mg, 0.83 mmol) and was directly used in the next step without any further purification. $R_f = 0.29$ ($CHCl_3$/MeOH 9:1).

**(*R*)-1-{3-[2-Oxo-3-(phenylamino)pyridin-1(2*H*)-yl]propanamido}-3-methylbutylboronic acid pinanediol ester (15l)**: According to the procedure described for **15a**, compound **15l** (230 mg, 77%) was obtained from acid **13l** (152 mg, 0.59 mmol) and was directly used in the next step without any further purification. $R_f = 0.59$ ($CHCl_3$/MeOH 9:1).

**(*R*)-1-{(*S*)-2-[2-Oxo-4-(phenylamino)pyridin-1(2*H*)-yl]-3-phenylpropanamido}-3-methylbutylboronic acid pinanediol ester (15m)**: According to the procedure described for **15b**, compounds **15m** (361 mg, 79%) and **5h** (69 mg, 22%) were obtained from acid **13m** (259 mg, 0.78 mmol). Compound **15m** was directly used in the next step without any further purification. $R_f = 0.49$ ($CHCl_3$/MeOH 9:1).

**(*R*)-1-{(*R*)-2-[2-Oxo-4-(phenylamino)pyridin-1(2*H*)-yl]-3-phenylpropanamido}-3-methylbutylboronic acid pinanediol ester (15n)**: According to the procedure described for **15a**, compound **15n** (354 mg, 70%) was obtained from acid **13n** (304 mg, 0.91 mmol) and was directly used in the next step without any further purification. $R_f = 0.49$ ($CHCl_3$/MeOH 9:1).

**(*R*)-1-{2-[4-(3-Ethylphenylamino)-2-oxopyridin-1(2*H*)-yl]acetamido}-3-methylbutylboronic acid (2a)**: A solution of **15a** (403 mg, 0.78 mmol) in MeOH/*n*-hexane (1:1, 30 mL) was treated with isobutylboronic acid (398 mg, 3.9 mmol) and 1 N HCl (1.95 mL). After 18 h at RT, the methanolic phase was washed with *n*-hexane (3× 10 mL) and the *n*-hexane layer was washed with MeOH (3×10 mL). The combined methanol phase was evaporated in vacuo. The residue was taken up into 5% $NaHCO_3$ (30 mL) and washed with $CH_2Cl_2$ (2×30 mL). The product was extracted with $CHCl_3$ (3× 30 mL), and the combined organic phase was dried with $Na_2SO_4$, filtered, and concentrated under reduced pressure. The crude product was purified by column chromatography ($CHCl_3$/$CH_3OH$ 9:1) to give **2a** (171 mg, 57%) as a white sticky solid. $R_f = 0.10$ ($CHCl_3$/MeOH 9:1). $[\alpha]_D^{20} = -11.5$ ($c = 0.1$, DMSO). $^1$H NMR (300 MHz, [$D_6$]DMSO): $\delta = 0.96$–$1.22$ (m, 9H), 1.31–1.70 (m, 3H), 2.56–2.66 (m, 2H), 2.98–3.04 (m, 1H), 4.50 (s, 2H), 5.89–5.95 (m, 2H), 6.82–7.10 ppm (m, 5H). $^{13}$C NMR (75 MHz, [$D_6$]DMSO): $\delta = 15.8$, 22.8, 26.2, 32.0, 32.3, 45.6, 51.9, 88.1, 111.1, 114.6, 123.9, 129.5, 135.0, 150.5, 156.1, 162.3, 167.0, 170.1 ppm. Elemental analysis calcd (%)

for $C_{20}H_{28}BN_3O_4$ (385.27): C 62.35, H 7.33, N 10.91; found: C 62.11, H 7.17, N 10.96.

**(*R*)-1-{2-[4-(4-Methoxyphenylamino)-2-oxopyridin-1(2*H*)-yl]acetamido}-3-methylbutylboronic acid (2b)**: Starting from **15b** (214 mg, 0.41 mmol), compound **2b** (94 mg, 59%) was obtained according to the procedure outlined for **2a**. $R_f$ = 0.13 ($CHCl_3$/MeOH 9:1). $[\alpha]_D^{20} = -6.7$ ($c$ = 0.1, DMSO). $^1$H NMR (300 MHz, [D$_6$]DMSO): $\delta$ = 0.73–0.90 (m, 6H), 1.14–1.75 (m, 3H), 3.30–3–34 (m, 1H), 3.73 (s, 3H), 4.31 (s, 2H), 5.45 (d, $J$ = 1.8 Hz, 1H), 5.82 (dd, $J$ = 7.0, 2.3 Hz, 1H), 6.90–7.10 ppm (m, 5H). $^{13}$C NMR (75 MHz, [D$_6$]DMSO): $\delta$ = 22.6, 22.8, 25.5, 29.5, 31.8, 45.7, 55.7, 114.9, 124.6, 133.1, 140.0, 154.6, 156.2, 162.8, 167.4, 167.7 ppm. Elemental analysis calcd (%) for $C_{19}H_{26}BN_3O_5$ (387.24): C 58.93, H 6.77, N 10.85; found: C 58.77, H 6.83, N 10.66.

**(*R*)-1-{2-[4-(Benzylamino)-2-oxopyridin-1(2*H*)-yl]acetamido}-3-methylbutylboronic acid (2c)**: Starting from **15c** (372 mg, 0.74 mmol), compound **2c** (187 mg, 68%) was obtained according to the procedure outlined for **2a**. $R_f$ = 0.12 ($CHCl_3$/MeOH 9:1). $[\alpha]_D^{20} = -2.7$ ($c$ = 0.1, DMSO). $^1$H NMR (300 MHz, [D$_6$]DMSO): $\delta$ = 0.78–0.87 (m, 6H), 1.05–1.28 (m, 3H), 3.01–3.08 (m, 1H), 4.18–4.4.26 (m, 4H), 5.51–5.54 (m, 1H), 5.55 (dd, $J$ = 7.5, 2.2 Hz, 1H), 7.07–7.35 ppm (m, 6H). $^{13}$C NMR (75 MHz, [D$_6$]DMSO): $\delta$ = 22.8, 23.3, 26.1, 32.3, 45.9, 76.7, 127.3, 127.6, 128.9, 139.2, 139.4, 156.4, 162.8, 170.1, 175.3 ppm. Elemental analysis calcd (%) for $C_{19}H_{26}BN_3O_4$ (371.24): C 61.47, H 7.06, N 11.32; found: C 61.73, H 7.01, N 11.44.

**(*R*)-1-{2-[2-Oxo-3-(phenylamino)pyridin-1(2*H*)-yl]acetamido}-3-methylbutylboronic acid (2d)**: Starting from **15d** (217 mg, 0.44 mmol), compound **2d** (79 mg, 50%) was obtained according to the procedure outlined for **2a**. $R_f$ = 0.11 ($CHCl_3$/MeOH 9:1). $[\alpha]_D^{20} = -13.7$ ($c$ = 0.1, DMSO). $^1$H NMR (300 MHz, [D$_6$]DMSO): $\delta$ = 0.86 (t, $J$ = 6.6 Hz, 6H), 1.28–1.72 (m, 3H), 3.39–3.44 (m, 1H), 4.57 (s, 2H), 6.27–6.33 (m, 1H), 6.97 (d, $J$ = 7.0 Hz, 1H), 7.08–7.37 ppm (m, 6H). $^{13}$C NMR (75 MHz, [D$_6$]DMSO): $\delta$ = 22.7, 25.5, 32.2, 44.4, 51.8, 89.1, 111.3, 116.7, 117.9, 129.4, 134.4, 153.3, 162.1, 170.1 ppm. Elemental analysis calcd (%) for $C_{18}H_{24}BN_3O_4$ (357.21): C 60.52, H 6.77, N 11.76; found: C 60.44, H 6.61, N 11.88.

**(*R*)-1-{2-[2-Oxo-3-(piperidin-1-yl)pyridin-1(2*H*)-yl]acetamido}-3-methylbutylboronic acid (2e)**: Starting from **15e** (430 mg, 0.89 mmol), compound **2e** (171 mg, 55%) was obtained according to the procedure outlined for **2a**. $R_f$ = 0.14 ($CHCl_3$/MeOH 9:1). $[\alpha]_D^{20} = -2.4$ ($c$ = 0.1, DMSO). $^1$H NMR (300 MHz, [D$_6$]DMSO): $\delta$ = 0.75–0.85 (m, 12H), 1.13–1.25 (m, 2H), 1.30–1.70 (m, 7H), 3.10–3.17 (m, 1H), 4.17 (s, 2H), 5.43 (s, 1H), 5.93- 0.03 (m, 1H), 7.20–7.24 ppm (m, 1H): $^{13}$C NMR (75 MHz, [D$_6$]DMSO): $\delta$ = 23.2, 26.0, 26.2, 26.5, 32.1, 44.3, 48.4, 51.8, 103.4, 111.8, 134.3, 147.5, 161.0, 167.0 173.5 ppm. Elemental analysis calcd (%) for $C_{17}H_{28}BN_3O_4$ (349.23): C 58.47, H 8.08, N 12.03; found: C 58.33, H 8.21, N 12.00.

**(*R*)-1-{3-[2-Oxopyridin-1(2*H*)-yl]propanamido}-3-methylbutylboronic acid (3a)**: Starting from **15f** (825 mg, 1.99 mmol), compound **3a** (206 mg, 37%) was obtained according to the procedure outlined for **2a**. $R_f$ = 0.15 ($CHCl_3$/MeOH 9:1). $[\alpha]_D^{20} = -6.7$ ($c$ = 0.03, DMSO). $^1$H NMR (300 MHz, $CD_3OD$): $\delta$ = 0.87 (d, $J$ = 6.6 Hz, 6H), 1.30 (m, 2H), 1.42–1.56 (m, 1H), 2.65 (t, $J$ = 6.6 Hz, 2H), 3.11–3.16 (m, 1H), 4.23 (t, $J$ = 6.6 Hz, 2H), 6.31–6.36 (m, 1H), 6.52 (d, $J$ = 8.4 Hz, 1H), 7.48–7.59 ppm (m, 2H). $^{13}$C NMR (75 MHz, [D$_6$]DMSO): $\delta$ = 23.3, 26.1, 32.1, 33.6, 44.3, 45.3, 111.4, 118.8, 134.1, 138.2, 161.5, 172.9 ppm. Elemental analysis calcd (%) for $C_{13}H_{21}BN_2O_4$ (280.13): C 55.74; H 7.56; N 10.00; found: C 55.27, H 7.63, N 10.11.

**(*R*)-1-{3-[2-Oxo-4-(phenylamino)pyridin-1(2*H*)-yl]propanamido}-3-methylbutylboronic acid (3b)**: Starting from **15g** (339 mg, 0.67 mmol), compound **3b** (137 mg, 55%) was obtained according to the procedure outlined for **2a**. $R_f$ = 0.10 ($CHCl_3$/MeOH 9:1). $[\alpha]_D^{20} = -13.5$ ($c$ = 0.2, DMSO). $^1$H NMR (300 MHz, [D$_6$]DMSO): $\delta$ = 0.80–0.87 (m, 6H), 1.20–1.56 (m, 3H), 2.41 (t, $J$ = 6.5 Hz, 2H), 3.14–3.21 (m, 1H), 3.91 (t, $J$ = 6.5 Hz, 2H), 5.71 (d, $J$ = 2.3 Hz, 1H), 5.88 (dd, $J$ = 7.0, 2.3 Hz, 1H), 7.04 (t, $J$ = 7.0 Hz, 1H), 7.13 (d, $J$ = 7.0 Hz, 2H), 7.30–7.35 ppm (m, 3H). $^{13}$C NMR (75 MHz, [D$_6$]DMSO): $\delta$ = 22.8, 25.4, 35.2, 37.0, 38.5, 45.2, 45.2, 94.1, 98.9, 121.5, 123.5, 129.7, 139.4, 140.6, 153.3, 162.7, 169.9 ppm. Elemental analysis calcd (%) for $C_{19}H_{26}BN_3O_4$ (371.24): C 61.47, H 7.06, N 11.32; found: C 61.29, H 7.22, N 11.01.

**(*R*)-1-{3-[4-(3-Ethylphenylamino)-2-oxopyridin-1(2*H*)-yl]propanamido}-3-methylbutylboronic acid (3c)**: Starting from **15h** (187 mg, 0.35 mmol), compound **3c** (98 mg, 70%) was obtained according to the procedure outlined for **2a**. $R_f$ = 0.11 ($CHCl_3$/MeOH 9:1). $[\alpha]_D^{20} = -17.1$ ($c$ = 0.1, DMSO). $^1$H NMR (300 MHz, [D$_6$]DMSO): $\delta$ = 0.79–0.89 (m, 9H), 1.13–1.29 (m, 3H), 2.39–2.44 (m, 2H), 2.57 (q, $J$ = 7.6 Hz, 2H), 2.98–3.05 (m, 1H), 3.88–4.03 (m, 2H), 5.69 (dd, $J$ = 6.5, 1.8 Hz, 1H), 5.86 (dd, $J$ = 7.0, 2.3 Hz, 1H), 6.87–6.96 (m, 3H), 7.18–7.34 ppm (m, 2H). $^{13}$C NMR (75 MHz, [D$_6$]DMSO): $\delta$ = 16.0, 22.8, 23.7, 24.1, 25.5, 28.6, 35.2, 38.1, 38.5, 93.9, 119.0, 121.1, 123.0, 129.5, 140.5, 145.4, 153.2, 153.5, 162.6, 169.8 ppm. Elemental analysis calcd (%) for $C_{21}H_{30}BN_3O_4$ (399.29): C 63.17, H 7.57, N 10.52; found: C 63.25; H 7.31; N 10.71.

**(*R*)-1-{3-[4-(4-Methoxyphenylamino)-2-oxopyridin-1(2*H*)-yl]propanamido}-3-methylbutylboronic acid (3d)**: Starting from **15i** (206 mg, 0.38 mmol), compound **3d** (101 mg, 66%) was obtained according to the procedure outlined for **2a**. $R_f$ = 0.13 ($CHCl_3$/MeOH 9:1). $[\alpha]_D^{20} = -13.3$ ($c$ = 0.1, DMSO). $^1$H NMR (300 MHz, [D$_6$]DMSO): $\delta$ = 0.85–0.89 (m, 6H), 1.23–1.47 (m, 3H), 2.29–2.33 (m, 2H), 2.98–3.05 (m, 1H), 3.70 (s, 3H), 4.11–4.23 (m, 2H), 5.71 (dd, $J$ = 7.0, 1.8 Hz, 1H), 5.99 (dd, $J$ = 7.0, 2.3 Hz, 1H), 6.94–7–27 ppm (m, 5H). $^{13}$C NMR (75 MHz, [D$_6$]DMSO): $\delta$ = 22.7, 22.9, 26.2, 32.1, 33.5, 45.8, 56.3, 88.4, 115.3, 127.3, 134.2, 143.6, 154.7, 157.3, 162.8, 168.7, 169.2 ppm. Elemental analysis calcd (%) for $C_{20}H_{28}BN_3O_5$ (401.27): C 59.87; H 7.03; N 10.47; found: C 59.88, H 7.01, N 10.73.

**(*R*)-1-{3-[2-Oxo-4-(piperidin-1-yl)pyridin-1(2*H*)-yl]propanamido}-3-methylbutylboronic acid (3e)**: Starting from **15j** (418 mg, 0.84 mmol), compound **3e** (204 mg, 69%) was obtained according to the procedure outlined for **2a**. $R_f$ = 0.11 ($CHCl_3$/MeOH 9:1). $[\alpha]_D^{20} = -3.9$ ($c$ = 0.1, DMSO). $^1$H NMR (300 MHz, $CD_3OD$): $\delta$ = 0.64–0.89 (m, 12H), 1.15–1.31 (m, 2H), 1.39–1.59 (m, 5H), 2.30–2.44 (m, 2H), 3.11–3.17 (m, 1H), 3.82–3.97 (m, 2H), 5.41 (s, 1H), 5.96–6.01 (m, 1H), 7.26–7.30 ppm (m, 1H). $^{13}$C NMR (75 MHz, [D$_6$]DMSO): $\delta$ = 23.3, 26.0, 26.3, 26.9, 32.0, 33.7, 44.4, 45.2, 48.7, 87.2, 111.3, 134.5, 161.3, 167.4, 173.6 ppm. Elemental analysis calcd (%) for $C_{18}H_{30}BN_3O_4$ (363.26): C 59.52, H 8.32, N 11.57; found: C 59.37, H 8.44, N 11.50.

**(*R*)-1-{3-[4-(4-Methylpiperazin-1-yl)-2-oxopyridin-1(2*H*)-yl]propanamido}-3-methylbutylboronic acid (3f)**: Starting from **15k** (308 mg, 0.60 mmol), compound **3f** (159 mg, 70%) was obtained according to the procedure outlined for **2a**. $R_f$ = 0.11 ($CHCl_3$/MeOH 9:1). $[\alpha]_D^{20} = -7.9$ ($c$ = 0.1, DMSO). $^1$H NMR (300 MHz, $CD_3OD$): $\delta$ = 0.85–0.93 (m, 6H), 1.27–1.51 (m, 3H), 2.33 (s, 3H), 2.52–2.54 (m, 4H), 2.59 (t, $J$ = 6.5 Hz, 2H), 2.98–3.01 (m, 1H), 3.19 (t, $J$ = 6.6 Hz, 2H), 3.36–3.38 (m, 4H), 5.70 (d, $J$ = 2.4 Hz, 1H), 6.20 (dd, $J$ = 7.9, 1.5 Hz, 1H), 7.33 ppm (d, $J$ = 7.9 Hz, 1H). $^{13}$C NMR (75 MHz, [D$_6$]DMSO): $\delta$ = 23.3, 26.1, 32.0, 35.6, 43.1, 44.7, 45.2, 50.7, 55.7, 86.8, 111.1, 134.5, 161.3, 166.9, 173.3 ppm. Elemental analysis calcd

(%) for $C_{17}H_{29}BN_4O_4$ (364.25): C 56.06, H 8.02, N 15.38; found: C 56.22, H 8.00, N 15.41.

**(*R*)-1-{3-[2-Oxo-3-(phenylamino)pyridin-1(2*H*)-yl]propanamido}-3-methylbutylboronic acid (3 g)**: Starting from **15 l** (230 mg, 0.45 mmol), compound **3 g** (75 mg, 45%) was obtained according to the procedure outlined for **2 a**. $R_f$ = 0.15 ($CHCl_3$/MeOH 9:1). $[\alpha]_D^{20} = -18.0$ ($c$ = 0.1, DMSO). $^1$H NMR (300 MHz, [$D_6$]DMSO): $\delta$ = 0.87 (t, $J$ = 6.6 Hz, 6H), 1.23–1.61 (m, 3H), 2.38 (t, $J$ = 6.5 Hz, 2H), 3.39–3.44 (m, 1H), 4.17 (t, $J$ = 6.5 Hz, 2H), 6.21–6.30 (m, 1H), 6.89 (d, $J$ = 7.0 Hz, 1H), 6.98–7.04 (m, 3H), 7.12–1.16 ppm (m, 2H). $^{13}$C NMR (75 MHz, [$D_6$]DMSO) $\delta$ = 23.1, 26.1, 32.3, 33.4, 44.7, 45.2, 105.8, 111.5, 116.5, 118.3, 129.6, 134.7, 140.2, 144.5, 158.6, 173.4 ppm. Elemental analysis calcd (%) for $C_{19}H_{26}BN_3O_4$ (371.24): C 61.47, H 7.06, N 11.32; found: C 61.31, H 7.26, N 11.22.

**(*R*)-1-{(*S*)-2-[2-Oxo-4-(phenylamino)pyridin-1(2*H*)-yl]-3-phenylpropanamido}-3-methylbutylboronic acid (4 a)**: Starting from **15 m** (361 mg, 0.62 mmol), compound **4 c** (161 mg, 58%) was obtained according to the procedure outlined for **2 a**. $R_f$ = 0.12 ($CHCl_3$/MeOH 9:1). $[\alpha]_D^{20} = -16.4$ ($c$ = 0.1, DMSO). $^1$H NMR (300 MHz, [$D_6$]DMSO): $\delta$ = 0.83–0.87 (m, 6H),1.13–1.56 (m 3H), 3.10–3.16 (m, 1H), 3.46–3.55 (m, 1H), 3.87–3.96 (m, 1H), 5.45–5.53 (m, 1H), 6.06–6.13 (m, 2H), 7.17–7.31 ppm (m, 11H). $^{13}$C NMR (75 MHz, [$D_6$]DMSO): $\delta$ = 22.9, 23.0, 24.4, 24.5, 25.2, 35.4, 44.5, 45.6, 47.3, 71.2, 94.6, 97.1, 138.8, 157.2, 162.7, 169.7 ppm. Elemental analysis calcd (%) for $C_{25}H_{30}BN_3O_4$ (447.34): C 67.12, H 6.76, N 9.39; found: C 67.09, H 6.78, N 9.27.

**(*R*)-1-{(*R*)-2-[2-Oxo-4-(phenylamino)pyridin-1(2*H*)-yl]-3-phenylpropanamido}-3-methylbutylboronic acid (4 b)**: Starting from **15 n** (354 mg, 0.64 mmol), compound **4 b** (151 mg, 53%) was obtained according to the procedure outlined for **2 a**. $R_f$ = 0.12 ($CHCl_3$/MeOH 9:1). $[\alpha]_D^{20} = +12.9$ ($c$ = 0.1, DMSO). $^1$H NMR (300 MHz, $CD_3OD$): $\delta$ = 0.82–0.88 (m, 6H),1.12–1.56 (m 3H), 3.13–3.19 (m, 1H), 3.44–3.52 (m, 1H), 3.99–4.07 (m, 1H), 5.33–5.46 (m, 1H), 6.11–6.18 (m, 2H), 7.21–7.33 ppm (m, 11H). $^{13}$C NMR (75 MHz, [$D_6$]DMSO): $\delta$ = 23.3, 26.1, 32.2, 35.6, 44.2, 46.5, 60.7, 116.2, 125.6, 126.4, 128.0, 128.5, 128.9, 129.3, 134.5, 138.8, 152.2, 161.4, 172.5 ppm. Elemental analysis calcd (%) for $C_{25}H_{30}BN_3O_4$ (447.34): C 67.12, H 6.76, N 9.39; found: C 67.23, H 6.62, N 9.44.

**Characterization of amides 5 a–h**

**2-[4-(4-Methoxyphenylamino)-2-oxo-2*H*-pyridin-1-yl]-*N*-isopentylacetamide (5 a)**: $R_f$ = 0.49 ($CHCl_3$/MeOH 95:5). $^1$H NMR (300 MHz, [$D_6$]DMSO): $\delta$ = 0.75–0.88 (m, 6H), 1.05–1.59 (m, 3H), 3.33–3.49 (m, 2H), 3.73 (s, 3H), 4.31 (s, 2H), 5.45 (d, $J$ = 1.8 Hz, 1H), 5.82 (dd, $J$ = 7.0, 2.3 Hz, 1H), 6.91–7.10 (m, 4H), 7.28 ppm (d, $J$ = 7.0 Hz, 1H). Elemental analysis calcd (%) for $C_{19}H_{25}N_3O_3$ (343.42): C 66.45, H 7.34, N 12.24; found: C 66.39, H 7.48, N 12.09.

***N*-Isopentyl-2-(2-oxo-3-phenylamino-2*H*-pyridin-1-yl)acetamide (5 b)**: $R_f$ = 0.59 ($CHCl_3$/MeOH 95:5). $^1$H NMR (300 MHz, [$D_6$]DMSO): $\delta$ = 0.81 (d, $J$ = 6.4 Hz, 6H), 1.21–1.61 (m, 3H), 2.95–3.07 (m, 2H), 4.11 (s, 2H), 6.11 (t, $J$ = 7.0 Hz, 1H), 6.89 (t, $J$ = 7.0 Hz, 1H), 6.99–7.25 ppm (m, 6H). Elemental analysis calcd (%) for $C_{18}H_{23}N_3O_2$ (313.39): C 68.98, H 7.40, N 13.41; found: C 68.77, H 7.55, N 10.09.

***N*-Isopentyl-2-(2′-oxo-3,4,5,6-tetrahydro-2*H*,2′*H*-[1,3′]bipyridinyl-1′-yl)acetamide (5 c)**: $R_f$ = 0.17 ($CHCl_3$/MeOH 95:5). $^1$H NMR (300 MHz, $CDCl_3$): $\delta$ = 0.84–0.94 (m, 6H), 1.18–1.76 (m, 13H), 3.02–3.05 (m, 2H), 4.67 (s, 2H), 6.19–6.24 (m, 2H), 7.51–7.54 ppm (m, 1H). Elemental analysis calcd (%) for $C_{17}H_{27}N_3O_2$ (305.42): C 66.85, H 8.91, N 13.76; found: C 66.79, H 8.99, N 13.54.

***N*-Isopentyl-3-(2-oxo-2*H*-pyridin-1-yl)propionamide (5 d)**: $R_f$ = 0.42 ($CHCl_3$/MeOH 95:5). $^1$H NMR (300 MHz, $CD_3OD$): $\delta$ = 0.86 (d, $J$ = 6.6 Hz, 6H), 1.29 (q, $J$ = 7.0 Hz, 2H), 1.42–1.56 (m, 1H), 2.65 (t, $J$ = 6.5 Hz, 2H), 3.14 (t, $J$ = 7.5 Hz, 2H), 4.23 (t, $J$ = 6.6 Hz, 2H), 6.29–6.37 (m, 1H), 6.52 (d, $J$ = 8.4 Hz, 1H), 7.44–7.58 ppm (m, 2H). Elemental analysis calcd (%) for $C_{13}H_{20}N_2O_2$ (236.31): C 66.07, H 8.53, N 11.85; found: C 67.09, H 8.44, N 11.87.

***N*-Isopentyl-3-(2-oxo-4-phenylamino-2*H*-pyridin-1-yl)propionamide (5 e)**: $R_f$ = 0.35 ($CHCl_3$/MeOH 95:5). $^1$H NMR (300 MHz, [$D_6$]DMSO): $\delta$ = 0.82 (d, $J$ = 6.4 Hz, 6H), 1.20–1.58 (m, 3H), 2.42 (t, $J$ = 6.4 Hz, 2H), 2.98–3.05 (m, 2H), 3.91 (t, $J$ = 6.4 Hz, 2H), 5.70 (d, $J$ = 2.3 Hz, 1H), 5.87 (dd, $J$ = 7.0, 2.3 Hz, 1H), 7.01–7.14 (m, 3H), 7.30–7.35 ppm (m, 3H). Elemental analysis calcd (%) for $C_{19}H_{25}N_3O_2$ (327.42): C 69.70, H 7.70, N 12.83; found: C 69.55, H 7.88, N 12.85.

***N*-Isopentyl-3-[4-(4-Methoxyphenylamino)-2-oxo-2*H*-pyridin-1-yl]propionamide (5 f)**: $R_f$ = 0.57 ($CHCl_3$/MeOH 9:1). $^1$H NMR (300 MHz, [$D_6$]DMSO): $\delta$ = 0.83–0.89 (m, 6H), 1.19–1.33 (m, 3H), 2.55–2.71 (m, 2H), 2.89–2.95 (m, 2H), 3.88 (s, 3H), 4.14–4.23 (m, 2H), 6.01 (d, $J$ = 1.8 Hz, 1H), 6.39 (dd, $J$ = 7.0, 2.3 Hz, 1H), 6.99–7–25 ppm (m, 5H). Elemental analysis calcd (%) for $C_{20}H_{27}N_3O_3$ (357.45): C 67.20, H 7.61, N 11.76; found: C 67.44, H 7.53, N 11.83.

***N*-Isopentyl-3-(2′-oxo-3,4,5,6-tetrahydro-2*H*,2′*H*-[1,4′]bipyridinyl-1′-yl)propionamide (5 g)**: $R_f$ = 0.34 ($CHCl_3$/MeOH 95:5). $^1$H NMR (300 MHz, [$D_6$]DMSO): $\delta$ = 0.77 (d, $J$ = 6.4 Hz, 6H), 1.15–1.30 (m, 3H), 1.39–1.59 (m, 10H), 3.13–3.27 (m, 3H), 3.84–3.96 (m, 2H), 5.41 (s, 1H), 5.99 (t, $J$ = 7.0 Hz, 1H), 7.26–7.30 ppm (m, 1H). Elemental analysis calcd (%) for $C_{18}H_{29}N_3O_2$ (319.44): C 67.68, H 9.15, N 13.15; found: C 67.77, H 9.07, N 13.31.

**(*S*)-*N*-Isopentyl-2-[2-oxo-4-(phenylamino)pyridin-1(2*H*)-yl]-3-phenylpropanamide (5 h)**: $R_f$ = 0.62 ($CHCl_3$/MeOH 9:1). $^1$H NMR (300 MHz, [$D_6$]DMSO): $\delta$ = 0.83–0.87 (m, 6H),1.07–1.46 (m 3H), 3.03–3.19 (m, 2H), 3.37–3.44 (m, 1H), 3.69–3.81 (m, 1H), 5.57–5.73 (m, 1H), 6.09–6.16 (m, 2H), 7.21–7.36 ppm (m, 11H). Elemental analysis calcd (%) for $C_{25}H_{29}N_3O_2$ (403.52): C 74.41, H 7.24, N 10.41; found: C 74.55, H 7.22, N 10.65.

### *Computational chemistry*

**General**: Molecular modeling and graphics manipulations were performed by using Maestro 9.2 (Schrödinger)[33] and UCSF-CHIMERA software packages[34] running on a E4 Computer Engineering E1080 workstation provided of a Intel Core i7-930 Quad-Core processor. GOLD 5.2[26,27] was used for all docking calculations. Figures were generated by using Pymol 1.0.[35]

**Protein and ligands preparation**: Coordinates for the ChT-L β5 subunit derived from the X-ray crystal structure of the yeast 20S proteasome determined at 2.8 Å resolution (PDB ID: 2F16)[13] were employed for the automated docking studies. The protein setup was performed by the Protein Preparation Wizard in Maestro.[31] Hydrogen atoms were added to the protein consistent with the neutral physiologic pH. Arginine and lysine side chains were considered as cationic at the guanidine and ammonium groups, and the aspartic and glutamic residues were considered as anionic at the carboxylate groups. The crystal structure of 20S/bortezomib complex revealed one well-defined water molecule in proximity to D114 $O^{\gamma}$, which coordinates a tight H-bonding network, interacting with β6-D114$O^{\gamma}$, β5-A49N, and β5-A50N of the protein and with the C=O oxygen atom of bortezomib.[13] Moreover, one of the pyrazine nitrogen atoms of bortezomib was found to interact through a direct H-bond with the protonated β6-D114. In fact, it has been observed that the p$K_a$ of pyrazine is approximately 1.0 and thus

β6-D114 is most likely protonated. This is supported by the fact that in the X-ray structure the O–N distance is 2.9 Å, which is indicative of a strong H-bond. Accordingly, the intervening water molecule and the proper protonation state of D114 were included in the docking experiments. The protonation and flip states of the imidazole rings of the histidine residues were adjusted together with the side chain amide groups of the glutamine and asparagine residues in a H-bonding network optimization process. Successively, the protein hydrogen atoms only were minimized by using the Impref module of Impact with the OPLS_2005 force field. The initial structures of **3c**, **3d**, **4c**, and **5h** were created, modified, and energy-minimized with Schrödinger's Maestro.[33]

**Docking studies**: Compounds **3c**, **3d**, and **4c** were covalently docked to the binding pocket of the β5 subunit by using GOLD 5.2.[26,27] For non-boronate-containing compound **5h**, a conventional docking procedure was performed. A radius of 20 Å from the β5 catalytic N-terminal threonine was used to direct site location. For each of the genetic algorithm runs, a maximum of 100000 operations was performed on a population of 100 individuals with a selection pressure of 1.1. Operator weights for crossover, mutation, and migration were set to 95, 95, and 10, respectively, as recommended by the authors of the software. The distance for H-bonding was set to 2.5 Å, and the cutoff value for van der Waals calculation was set to 4 Å. Covalent docking was applied, and the terminal boron atom of **3c**, **3d**, and **4c** was bonded to the hydroxyl oxygen atom of β5-T1. The water molecule near β6-D114 (crystallographically determined for the proteasome/bortezomib complex) was specified in GOLD by switching state settings to "toggle" and orientation mode to "spin". The Goldscore-CS docking protocol[36] was adopted in this study. In this protocol, the poses obtained with the original GoldScore function are rescored and reranked with the GOLD implementation of the ChemScore function.[6,36–39] To perform thorough and unbiased search of the conformation space, each docking run was allowed to produce 200 poses without the option of early termination by using standard default settings. The top solution obtained after reranking of the poses with ChemScore was selected to generate the proteasome/ligand complexes.

### *Biology*

*In vitro 20S proteasome inhibition assays*: Human 20S proteasome was obtained from Biomol GmbH, Hamburg, Germany. The three distinct proteolytic activities of the 20S proteasome were measured by monitoring the hydrolysis of the peptidyl 7-amino-4-methyl coumarin substrates (all obtained from Bachem) Suc-Leu-Leu-Val-Tyr-AMC, Boc-Leu-Arg-Arg-AMC, and Cbz-Leu-Leu-Glu-AMC for ChT-L, T-L, and PGPH activity of the enzyme, respectively. Fluorescence of the product AMC of the substrates' hydrolyses was measured by using an Infinite 200 PRO microplate reader (Tecan, Männedorf, Switzerland) at 30 °C with a 380 nm excitation filter and a 460 nm emission filter. The preliminary screening for the inhibition of the three proteolytic activities of the 20S proteasome was performed at 20 μM inhibitor concentrations by using an equivalent amount of DMSO as a negative control. Compounds showing at least 40% inhibition at 20 μM were subjected to detailed assays. The dissociation constants $K_i$ of the noncovalent complex E·I were obtained from progress curves (10 min) at various concentrations of inhibitor by fitting the progress curves to a four-parameter $IC_{50}$ equation and correction to zero substrate concentration by using Equation (1). The $K_m$ values were determined in separate experiments: ChT-L activity with Suc-Leu-Leu-Val-Tyr-AMC 13 μM and PGPH activity with Cbz-Leu-Leu-Glu-AMC 53 μM.

$$K_i = \frac{IC_{50}}{1 + [S]K_m^{-1}} \quad (1)$$

in which [S] is the fixed substrate concentration and $K_m$ is the concentration of the substrate at which enzyme activity is half maximal.

*Assaying the chymotryptic activity of the 20S proteasome*: Human 20S proteasome was incubated at 30 °C at a final concentration of 0.004 mg mL$^{-1}$ with test compound present at variable concentrations. The reaction buffer consisted of 50 mM tris(hydroxymethyl)aminomethane (Tris) pH 7.5, 10 mM NaCl, 25 mM KCl, 1 mM $MgCl_2$, 0.03% sodium dodecyl sulfate (SDS), and 5% DMSO. Product released from substrate hydrolysis (75 μM) was monitored continuously over a period of 10 min.

*Assaying the tryptic activity of the 20S proteasome*: Human 20S proteasome was incubated at 30 °C at a final concentration of 0.0025 mg mL$^{-1}$ with test compound present at 20 μM. The reaction buffer consisted of 50 mM Tris buffer pH 7.4, 50 mM NaCl, 0.5 mM ethylenediaminetetraacetic acid (EDTA), 0.03% SDS, and 7.5% DMSO. Product released from substrate hydrolysis (85 μM) was monitored continuously over a period of 10 min.

*Assaying the post glutamyl peptide hydrolyzing activity of the 20S proteasome*: Human 20S proteasome was incubated at 30 °C at a final concentration of 0.004 mg mL$^{-1}$ with the test compound present at variable concentrations. The reaction buffer consisted of 50 mM Tris buffer pH 7.5 containing 25 mM KCl, 10 mM NaCl, 1 mM $MgCl_2$, 0.03% SDS, 5% DMSO. Product released from substrate hydrolysis (80 μM) was monitored continuously over a period of 10 min.

*Assays for bovine pancreatic α-chymotrypsin inhibition*: The enzyme (250 μg mL$^{-1}$) was incubated at 20 °C with test compound. The reaction buffer consisted of 50 mM Tris buffer pH 8.0 containing 100 mM NaCl and 5 mM EDTA and 7.5% DMSO. Product released from substrate hydrolysis (75 μM final concentration, Suc-Leu-Leu-Val-Tyr-AMC from Bachem) was determined over a period of 10 min.

## *Acknowledgements*

*This work was financially supported by the Italian Ministry of Education, Universities and Research (MIUR) [MIUR-PRIN2010-2011, grants 2010W7YRLZ_003 (A.L.) and 2010W7YRLZ_004 (S.G.)]. The authors would like to thank the German Academic Exchange Service (DAAD) (Vigoni project 2011/12) for partial support of this work. T.S. thanks the German Research Foundation (DFG) for financial support. R.E. acknowledges the support of her postdoctoral fellowship from "Dote Ricerca": FSE, Regione Lombardia. The authors also thank the US National Cancer Institute, Division of Cancer Research (Bethesda, Maryland, USA) for performing the antitumor tests.*

**Keywords:** anticancer agents · boronates · bortezomib · docking studies · inhibitors · peptidomimetics · proteasomes

[1] N. Micale, K. Scarbaci, V. Troiano, R. Ettari, S. Grasso, M. Zappalà, *Med. Res. Rev.* **2014**, DOI: 10.1002/med.21312.
[2] M. Groll, W. Heinemeyer, S. Jager, T. Ulrich, M. Bochtler, D. H. Wolf, R. Huber, *Proc. Natl. Acad. Sci. USA* **1999**, *96*, 10976 – 10983.

[3] A. Sacco, M. Aujay, B. Morgan, A. K. Aza, P. Mais, Y. Liu, Y. Zhang, F. Azab, H. T. Ngo, G. C. Issa, P. Quang, A. M. Roccaro, I. M. Ghobria, *Clin. Cancer Res.* **2011**, *17*, 1753 – 1764.
[4] A. F. Kisselev, A. Callard, A. L. Goldberg, *J. Biol. Chem.* **2006**, *281*, 8582 – 8590.
[5] R. Ettari, C. Bonaccorso, N. Micale, C. Heindl, T. Schirmeister, M. L. Calabrò, S. Grasso, M. Zappalà, *ChemMedChem* **2011**, *6*, 1228 – 1237.
[6] N. Micale, R. Ettari, A. Lavecchia, C. Di Giovanni, K. Scarbaci, V. Troiano, S. Grasso, E. Novellino, T. Schirmeister, M. Zappalà, *Eur. J. Med. Chem.* **2013**, *64*, 23 – 34.
[7] A. Field-Smith, G. J. Morgan, F. E. Davies, *Ther. Clin. Risk Manage.* **2006**, *2*, 271 – 279.
[8] R. C. Kane, R. Dagher, A. Farrell, C. W. Ko, R. Sridhara, R. Justice, R. Pazdur, *Clin. Cancer Res.* **2007**, *13*, 5291 – 5294.
[9] M. Groll, R. Huber, L. Moroder, *J. Pept. Sci.* **2009**, *15*, 58 – 66.
[10] a) N. Micale, A. P. Kozikowski, R. Ettari, S. Grasso, M. Zappalà, J.-J. Jeong, A. Kumar, M. Hanspal, A. H. Chishti, *J. Med. Chem.* **2006**, *49*, 3064 – 3067; b) R. Ettari, E. Nizi, M. E. Di Francesco, M. A. Dude, G. Pradel, R. Vicik, T. Schirmeister, N. Micale, S. Grasso, M. Zappalà, *J. Med. Chem.* **2008**, *51*, 988 – 996; c) R. Ettari, E. Nizi, M. E. Di Francesco, N. Micale, S. Grasso, M. Zappalà, R. Vičík, T. Schirmeister, *ChemMedChem* **2008**, *3*, 1030 – 1033; d) R. Ettari, N. Micale, T. Schirmeister, C. Gelhaus, M. Leippe, E. Nizi, M. E. Di Francesco, S. Grasso, M. Zappalà, *J. Med. Chem.* **2009**, *52*, 2157 – 2160.
[11] a) R. Ettari, M. Zappalà, N. Micale, T. Schirmeister, C. Gelhaus, M. Leippe, A. Evers, S. Grasso, *Eur. J. Med. Chem.* **2010**, *45*, 3228 – 3233; b) R. Ettari, N. Micale, G. Grazioso, F. Bova, T. Schirmeister, S. Grasso, M. Zappalà, *ChemMedChem* **2012**, *7*, 1594 – 1600.
[12] a) R. Ettari, L. Tamborini, I. C. Angelo, S. Grasso, T. Schirmeister, L. Lo Presti, C. De Micheli, A. Pinto, P. Conti, *ChemMedChem* **2013**, *8*, 2070 – 2076; b) G. Grazioso, L. Legnani, L. Toma, R. Ettari, N. Micale, C. De Micheli, *J. Comput.-Aided Mol. Des.* **2012**, *26*, 1035 – 1043.
[13] a) M. Groll, C. R. Berkers, H. L. Ploegh, H. Ovaa, *Structure* **2006**, *14*, 451 – 456; b) M. Groll, L. Ditzel, J. Löwe, D. Stock, M. Bochtler, H. D. Bartunik, R. Huber, *Nature* **1997**, *386*, 463 – 471.
[14] Y. Zhu, G. Wu, X. Zhu, Y. Ma, X. Zhao, Y. Li, Y. Yuan, J. Yang, S. Yu, F. Shao, M. Lei, *J. Med. Chem.* **2010**, *53*, 8619 – 8626.
[15] Y. Zhu, X. Zhu, G. Wu, Y. Ma, Y. Li, X. Zhao, Y. Yuan, J. Yang, S. Yu, F. Shao, R. Li, Y. Ke, A. Lu, Z. Liu, L. Zhang, *J. Med. Chem.* **2010**, *53*, 1990 – 1999.
[16] a) R. Ettari, L. Tamborini, I. C. Angelo, N. Micale, A. Pinto, C. De Micheli, P. Conti, *J. Med. Chem.* **2013**, *56*, 5637 – 5658; b) R. Ettari, F. Bova, M. Zappalà, S. Grasso, N. Micale, *Med. Res. Rev.* **2010**, *30*, 136 – 167.
[17] R. Ettari, M. Zappalà, N. Micale, G. Grazioso, S. Giofrè, T. Schirmeister, S. Grasso, *Eur. J. Med. Chem.* **2011**, *46*, 2058 – 2065.
[18] F. Bova, R. Ettari, N. Micale, C. Carnovale, T. Schirmeister, C. Gelhaus, M. Leippe, S. Grasso, M. Zappalà, *Bioorg. Med. Chem.* **2010**, *18*, 4928 – 4938.
[19] N. Micale, R. Ettari, T. Schirmeister, A. Evers, C. Gelhaus, M. Leippe, M. Zappalà, S. Grasso, *Bioorg. Med. Chem.* **2009**, *17*, 6505 – 6511.
[20] A. Rentsch, D. Landsberg, T. Brodmann, L. Bülow, A. K. Girbig, M. Kalesse, *Angew. Chem.* **2013**, *125*, 5560 – 5599; *Angew. Chem. Int. Ed.* **2013**, *52*, 5450 – 5488.
[21] L. Borissenko, M. Groll, *Chem. Rev.* **2007**, *107*, 687 – 717.
[22] K. Scarbaci, V. Troiano, N. Micale, R. Ettari, C. Di Giovanni, C. Cerchia, S. Grasso, E. Novellino, T. Schirmeister, A. Lavecchia, M. Zappalà, *Eur. J. Med. Chem.* **2014**, *76*, 1 – 9.
[23] M. L. Stein, H. Cui, P. Beck, C. Dubiella, C. Voss, A. Krüger, B. Schmidt, M. Groll, *Angew. Chem.* **2014**, *126*, 1705 – 1709; *Angew. Chem. Int. Ed.* **2014**, *53*, 1679 – 1683.
[24] Y. H. Kim, Y.-J. Kim, S.-Y. Chang, B. T. Kim, J.-N. Heo, *Bull. Korean Chem. Soc.* **2007**, *28*, 777 – 782.
[25] J. R. Johnson, M. G. Van Campen, Jr., O. Grummit, *J. Am. Chem. Soc.* **1938**, *60*, 111 – 115.
[26] G. Jones, P. Willett, R. C. Glen, A. R. Leach, R. Taylor, *J. Mol. Biol.* **1997**, *267*, 727 – 748.
[27] GOLD, version 5.2, The Cambridge Crystallographic Data Centre, Cambridge, U.K., **2012**.
[28] Y. Q. Zhu, X. Zhao, X. R. Zhu, G. Wu, Y. J. Li, Y. H. Ma, Y. X. Yuan, J. Yang, Y. Hu, L. Ai, Q. Z. Gao, *J. Med. Chem.* **2009**, *52*, 4192 – 4199.
[29] R. M. Rydzewski, L. Burrill, R. Mendonca, J. T. Palmer, M. Rice, R. Tahilramani, K. E. Bass, L. Leung, E. Gjerstad, J. W. Janc, L. Pan, *J. Med. Chem.* **2006**, *49*, 2953 – 2296.
[30] E. M. Huber, M. Basler, R. Schwab, W. Heinemeyer, C. J. Kirk, M. Groettrup, M. Groll, *Cell* **2012**, *148*, 727 – 738.
[31] M. R. Boyd, K. D. Paull, *Drug Dev. Res.* **1995**, *34*, 91 – 109.
[32] M. R. Boyd, *Anticancer Drug Development Guide: Preclinical Screening, Clinical Trials, and Approval* (Ed.: B. A. Teicher), Humana Press, Totowa, NJ, **1997**, p. 23.
[33] Maestro, version 9.2, Schrödinger, LLC, New York, NY, **2013**.
[34] C. C. Huang, G. S. Couch, E. F. Pettersen, T. E. Ferrin, *Pac. Symp. Biocomput.* **1996**, *1*, 724; http://www.cgl.ucsf.edu/chimera.
[35] The PyMOL Molecular Graphics System, version 1.0, Schrödinger, LLC, San Carlos, CA. http://www.pymol.org.
[36] M. L. Verdonk, J. C. Cole, M. J. Hartshorn, C. W. Murray, R. D. Taylor, *Proteins Struct. Funct. Genet.* **2003**, *52*, 609 – 623.
[37] G. Fracchiolla, A. Laghezza, L. Piemontese, P. Tortorella, F. Mazza, R. Montanari, G. Pochetti, A. Lavecchia, E. Novellino, S. Pierno, D. C. Camerino, F. Loiodice, *J. Med. Chem.* **2009**, *52*, 6382 – 6393.
[38] L. Porcelli, F. Gilardi, A. Laghezza, L. Piemontese, N. Mitro, A. Azzariti, F. Altieri, L. Cervoni, G. Fracchiolla, M. Giudici, U. Guerrini, A. Lavecchia, R. Montanari, C. Di Giovanni, A. Paradiso, G. Pochetti, G. M. Simone, P. Tortorella, M. Crestani, F. Loiodice, *J. Med. Chem.* **2012**, *55*, 37 – 54.
[39] M. G. Perrone, P. Vitale, P. Malerba, A. Altomare, A. Lavecchia, C. Di Giovanni, E. Novellino, A. Scilimati, *ChemMedChem* **2012**, *7*, 629 – 641.

Received: March 19, 2014
Published online on May 28, 2014